

# Particle-Antiparticle Mixing, $\varepsilon_K$ , $\Delta\Gamma_q$ , $A_{\text{SL}}^q$ , $A_{\text{CP}}(B_d \rightarrow \psi K_S)$ , $A_{\text{CP}}(B_s \rightarrow \psi\phi)$ and $B \rightarrow X_{s,d}\gamma$ in the Littlest Higgs Model with T-Parity

Monika Blanke, Andrzej J. Buras, Anton Poschenrieder,  
Cecilia Tarantino, Selma Uhlig and Andreas Weiler

*Physik Department, Technische Universität München, D-85748 Garching, Germany*

## Abstract

We calculate a number of observables related to particle-antiparticle mixing in the Littlest Higgs model with T-parity (LHT). The resulting effective Hamiltonian for  $\Delta F = 2$  transitions agrees with the one of Hubisz et al., but our phenomenological analysis goes far beyond the one of these authors. In particular, we point out that the presence of mirror fermions with new flavour and CP-violating interactions allows to remove the possible Standard Model (SM) discrepancy between the CP asymmetry  $S_{\psi K_S}$  and large values of  $|V_{ub}|$  and to obtain for the mass difference  $\Delta M_s < (\Delta M_s)_{\text{SM}}$  as suggested by the recent result by the CDF collaboration. We also identify a scenario in which simultaneously significant enhancements of the CP asymmetries  $S_{\psi\phi}$  and  $A_{\text{SL}}^q$  relative to the SM are possible, while satisfying all existing constraints, in particular from the  $B \rightarrow X_s\gamma$  decay and  $A_{\text{CP}}(B \rightarrow X_s\gamma)$  that are presented in the LHT model here for the first time. In another scenario the second, non-SM, value for the angle  $\gamma = -(109 \pm 16)^\circ$  from tree level decays, although unlikely, can be made consistent with all existing data with the help of mirror fermions. We present a number of correlations between the observables in question and study the implications of our results for the mass spectrum and the weak mixing matrix of mirror fermions. In the most interesting scenarios, the latter one turns out to have a hierarchical structure that differs significantly from the CKM one.

# 1 Introduction

One of the most important messages that will be hopefully provided in the coming years by LHC and later by ILC is the detailed information about the electroweak symmetry breaking (EWSB) and the origin of the hierarchy of quark masses and their hierarchical flavour and CP-violating interactions. While supersymmetry [1] appears at present to be the leading candidate for a self-consistent incorporation of the Higgs mechanism into the framework of gauge theories, recent proposals like Little Higgs models [2, 3], Extra dimension models [4, 5], gauge-Higgs unification models [6, 7] and improved versions of technicolour [8, 9] and top colour [10] have still potential to provide at least partial solutions to EWSB and to shed light on the hierarchical structure of flavour violating interactions. Each of these proposals introduces new particles below 1 TeV or slightly above it with often significant impact of their contributions on electroweak precision studies and FCNC processes.

Among the most popular non-supersymmetric models in question are the Little Higgs models of which the so-called Littlest Higgs model [11] has been studied most extensively in the literature (see [3] and references therein). In this model in addition to the Standard Model (SM) particles, new charged heavy vector bosons ( $W_H^\pm$ ), a neutral heavy vector boson ( $Z_H^0$ ), a heavy photon ( $A_H$ ), a heavy top quark ( $T_+$ ) and a triplet of scalar heavy particles ( $\Phi$ ) are present.

In the original Littlest Higgs model (LH), the custodial  $SU(2)$  symmetry, of fundamental importance for electroweak precision studies, is unfortunately broken already at tree level, implying that the relevant scale of new physics,  $f$ , must be at least  $2 - 3$  TeV in order to be consistent with electroweak precision data [12]-[18]. As a consequence the contributions of the new particles to FCNC processes turn out to be at most 10–20% [19]-[22], which will not be easy to distinguish from the SM in view of experimental and theoretical uncertainties.

More promising and more interesting from the point of view of FCNC processes is the Littlest Higgs model with a discrete symmetry (T-parity) [23] under which all new particles listed above, except  $T_+$ , are odd and do not contribute to processes with external SM quarks (even under T-parity) at tree level. As a consequence the new physics scale  $f$  can be lowered down to 1 TeV and even below it, without violating electroweak precision constraints [24].

A consistent and phenomenologically viable Littlest Higgs model with T-parity (LHT) requires the introduction of three doublets of “mirror quarks” and three doublets of “mirror leptons” which are odd under T-parity, transform vectorially under  $SU(2)_L$  and can be given a large Dirac mass. Moreover, there is an additional heavy  $T_-$  quark that

is also odd under T-parity [25].<sup>1</sup>

In the first phenomenological studies of the LHT model [27] the contributions of mirror fermions to physical observables have not been considered, while their impact on electroweak precision tests has been investigated in [24]. More recently, in an interesting paper by Hubisz et al. [28] the role of mirror fermions in neutral meson mixing in the  $K$ ,  $B$  and  $D$  systems has been studied in some detail. The main messages of [28] are:

- There are new flavour violating interactions in the mirror quark sector, which can be parametrized by two CKM-like mixing matrices  $V_{Hd}$  and  $V_{Hu}$ , relevant for the processes with external light down-type quarks and up-type quarks, respectively. These two matrices are related through  $V_{Hu}^\dagger V_{Hd} = V_{\text{CKM}}$ . Similar comments apply to the mirror lepton sector.
- The spectrum of mirror quarks must be generally quasi-degenerate, if  $\mathcal{O}(1)$  mixing angles are allowed in the new mixing matrices, but there exist regions of parameter space, where only a loose degeneracy is necessary in order to satisfy constraints coming from particle-antiparticle mixing.

The recent measurements of the  $B_s^0 - \bar{B}_s^0$  mass difference  $\Delta M_s$  by the CDF and DØ collaborations [29, 30], that turns out to be close to the SM value, puts clearly an additional constraint on the model in question.

In the present paper we confirm the analytic expressions for the effective Hamiltonians for  $K^0 - \bar{K}^0$ ,  $B_d^0 - \bar{B}_d^0$  and  $B_s^0 - \bar{B}_s^0$  mixings presented in [28] and we generalize the analysis of these authors to other quantities that allow a deeper insight into the flavour structure of the LHT model. However, before listing the new aspects of our paper relatively to [28], let us emphasize a few points about the model in question that have not been stated so far in the literature.

While the original LH model belongs to the class of models with Minimal Flavour Violation (MFV) [31]-[33], this is certainly not the case of the LHT model where the presence of the matrices  $V_{Hd}$  and  $V_{Hu}$  in the mirror quark sector introduces new flavour and CP-violating interactions that could have a very different pattern from the ones present in the SM.

One should also emphasize that the manner in which the LHT model goes beyond the MFV scenario differs from the frameworks studied in [34] and [35], where the modification of the flavour structure is connected dominantly to the third generation of quarks. Here, the new flavour violating interactions come simply from another sector that couples

---

<sup>1</sup>In [26], an alternative way of implementing T-parity in the top sector has been proposed, where  $T_+$  is absent.

weakly to ordinary fermions and in principle all generations of mirror fermions can contribute to FCNC processes with equal strength.

The beauty of this model, when compared with other models with non-minimal flavour violating interactions, like general MSSM, is a relatively small number of new parameters and the fact that the local operators involved are the same as in the SM. Therefore the non-perturbative uncertainties, present in certain quantities already in the SM, are the same in the LHT model. Consequently the departures from the SM are entirely due to short distance physics that can be calculated within perturbation theory. In stating this we are aware of the fact that we deal here with an effective field theory whose ultraviolet completion has not been specified, with the consequence that at a certain level of accuracy one has to worry about the effects coming from the cut-off scale  $\Lambda \sim 4\pi f$ . We will assume that in the case of particle-antiparticle mixing and  $B \rightarrow X_s \gamma$  such effects are small.

So what is new in our paper relatively to [28]?

- While the authors of [28] analyzed only the mass differences  $\Delta M_K$ ,  $\Delta M_d$ ,  $\Delta M_s$ ,  $\Delta M_D$  and the CP violating parameter  $\varepsilon_K$ , we include in our analysis also the CP asymmetries  $A_{\text{CP}}(B_d \rightarrow \psi K_S)$ ,  $A_{\text{CP}}(B_s \rightarrow \psi \phi)$  and  $A_{\text{SL}}^q$ , and the width difference  $\Delta\Gamma_q$ , that are theoretically cleaner than the quantities considered in [28].
- Equally important, we present for the first time the expressions for the  $B \rightarrow X_{s,d}\gamma$  decay within the LHT model. As  $B \rightarrow X_s \gamma$  has played already an important role in constraining other extensions of the SM and is experimentally measured with good accuracy, it is mandatory to study it in the LHT model as well. In this context we also calculate the corresponding CP asymmetries.
- Our analysis of the mixing induced CP asymmetries  $A_{\text{CP}}(B_d \rightarrow \psi K_S)$  and  $A_{\text{CP}}(B_s \rightarrow \psi \phi)$  illustrates very clearly that with mirror fermions at work these asymmetries do *not* measure the phases  $-\beta$  and  $-\beta_s$  of the CKM elements  $V_{td}$  and  $V_{ts}$ , respectively.
- This has two interesting consequences: first, the possible “discrepancy” between the values of  $\sin 2\beta$  following directly from  $A_{\text{CP}}(B_d \rightarrow \psi K_S)$  and indirectly from the usual analysis of the unitarity triangle involving  $\Delta M_q$ ,  $\varepsilon_K$  and  $|V_{ub}/V_{cb}|$  can be avoided within the LHT model. Second, the asymmetries  $A_{\text{CP}}(B_s \rightarrow \psi \phi)$  and  $A_{\text{SL}}^q$  can be significantly enhanced over the SM expectations.
- In connection with the recent measurement of  $\Delta M_s$  by the CDF collaboration [29], that although close to the SM value, is somewhat lower than expected, we

investigate for which set of parameters of the LHT model  $\Delta M_s$  can be lower than  $(\Delta M_s)_{\text{SM}}$  while simultaneously solving the “ $\sin 2\beta$ ” problem mentioned above.

- We also find that the usual relation between  $\Delta M_d/\Delta M_s$  and  $|V_{td}/V_{ts}|$  characteristic for all models with MFV is no longer satisfied.
- We introduce the concept of the “mirror unitarity triangle” which could turn out to be useful once the analysis will be generalized in [36] to include rare  $K$  and  $B$  decays.
- We also investigate whether the second, non-MFV, solution for  $\gamma = -109^\circ$  from tree level decays can be made consistent with all available data.
- Finally, we present explicit formulae for the contributions of the T-even sector, that in the model in question are entirely dominated by the contributions of the heavy  $T_+$  quark. We emphasize that these contributions cannot be neglected for values of the parameter  $x_L > 0.5$  and in the limit of exactly degenerate mirror fermions constitute the only new contributions in this model.

Our paper is organized as follows. In Section 2 we summarize those ingredients of the LHT model that are of relevance for our analysis and we introduce mirror unitarity triangles. Section 3 is devoted to the particle-antiparticle mixings,  $\varepsilon_K$ , the asymmetries  $A_{\text{CP}}(B_d \rightarrow \psi K_S)$ ,  $A_{\text{CP}}(B_s \rightarrow \psi \phi)$ ,  $A_{\text{SL}}^q$ , the width differences  $\Delta\Gamma_q$  and in particular to the ratio  $\Delta M_d/\Delta M_s$ . We collect in this section a number of formulae that should be useful also for other models. In Section 4 we calculate the branching ratios for  $B \rightarrow X_s \gamma$  and  $B \rightarrow X_d \gamma$  and the corresponding CP asymmetries. In Section 5 we outline our strategy and our goals for the numerical analysis of Section 7. In Section 6 we discuss the benchmark scenarios for the parameters of the LHT model, which we explore in Section 7, where the correlations between various observables can be studied more explicitly than it is possible in the recent model independent analyses in [35, 37]-[43]. It is in this section where we address the possible discrepancy between the indirect and direct determinations of the angle  $\beta$  in the UT, its resolution within the LHT model, the enhancements of  $A_{\text{CP}}(B_s \rightarrow \psi \phi)$  and  $A_{\text{SL}}^q$  and the size of the corrections to the MFV result for  $\Delta M_d/\Delta M_s$ . A highlight of this section is also the analysis of the mirror fermion contributions to  $\Delta M_s$  in view of the recent measurements of  $B_s^0 - \bar{B}_s^0$  mixing [29, 30] and its possible correlation with  $Br(B \rightarrow X_s \gamma)$ . Also the rescue of the non-SM solution for  $\gamma$  with the help of mirror fermions is demonstrated in this section. In Section 8 we discuss briefly the  $D^0 - \bar{D}^0$  mixing. Finally, in Section 9 we conclude our paper with a list of messages resulting from our analysis and with a brief outlook. Few technical details are relegated to the Appendices.

## 2 General Structure of the LHT Model

A detailed description of the LHT model can be found e.g. in [27]. Here we just want to state briefly the ingredients needed for our analysis.

### 2.1 Gauge Boson Sector

#### 2.1.1 T-even Sector

The T-even electroweak gauge boson sector [11] consists only of SM electroweak gauge bosons

$$W_L^\pm, \quad Z_L, \quad A_L, \quad (2.1)$$

with masses given to lowest order in  $v/f$  by

$$M_{W_L} = \frac{gv}{2}, \quad M_{Z_L} = \frac{M_{W_L}}{\cos \theta_W}, \quad M_{A_L} = 0, \quad (2.2)$$

where  $\theta_W$  is the weak mixing angle. T-parity ensures that the second relation in (2.2) is satisfied at tree level to all orders in  $v/f$ . Only  $W_L^\pm$  will be present in the discussion of  $\Delta F = 2$  processes while both  $A_L$  and  $W_L^\pm$  enter the  $B \rightarrow X_s \gamma$  decay.

#### 2.1.2 T-odd Sector

The T-odd gauge boson sector [11] consists of three heavy “partners” of the SM gauge bosons in (2.1):

$$W_H^\pm, \quad Z_H, \quad A_H, \quad (2.3)$$

with masses given to lowest order in  $v/f$  by

$$M_{W_H} = gf, \quad M_{Z_H} = gf, \quad M_{A_H} = \frac{g'f}{\sqrt{5}}. \quad (2.4)$$

All three gauge bosons will be present in our analysis. Note that

$$M_{A_H} = \frac{\tan \theta_W}{\sqrt{5}} M_{W_H} \simeq \frac{M_{W_H}}{4.1}. \quad (2.5)$$

### 2.2 Fermion Sector

#### 2.2.1 T-even Sector

The T-even fermion sector [11] consists of the SM quarks and leptons and a colour triplet heavy quark  $T_+$  that is, to leading order in  $v/f$ , singlet under  $SU(2)_L$  and has the mass

$$m_{T_+} = \frac{f}{v} \frac{m_t}{\sqrt{x_L(1-x_L)}}, \quad x_L = \frac{\lambda_1^2}{\lambda_1^2 + \lambda_2^2}. \quad (2.6)$$

Here  $\lambda_1$  is the Yukawa coupling in the  $(t, T_+)$  sector and  $\lambda_2$  parametrizes the mass term of  $T_+$ .

### 2.2.2 T-odd Sector

The T-odd fermion sector [25] consists first of all of three generations of mirror quarks and leptons with vectorial couplings under  $SU(2)_L$ . In this paper only mirror quarks are relevant. We will denote them by

$$\begin{pmatrix} u_H^1 \\ d_H^1 \end{pmatrix}, \quad \begin{pmatrix} u_H^2 \\ d_H^2 \end{pmatrix}, \quad \begin{pmatrix} u_H^3 \\ d_H^3 \end{pmatrix}, \quad (2.7)$$

with their masses satisfying to first order in  $v/f$

$$m_{H1}^u = m_{H1}^d, \quad m_{H2}^u = m_{H2}^d, \quad m_{H3}^u = m_{H3}^d. \quad (2.8)$$

The T-odd fermion sector contains also a T-odd heavy quark  $T_-$ , which will not enter our analysis for reasons given in Appendix A. For completeness, we quote the expression for its mass,

$$m_{T_-} = \lambda_2 f = \frac{f}{v} \frac{m_t}{\sqrt{x_L}}. \quad (2.9)$$

In principle a lower bound on  $m_{T_-}$  like  $m_{T_-} > 500$  GeV could set an upper bound on  $x_L$  for fixed  $f$ , but it turns out that the electroweak precision constraints are more important [24].

### 2.3 Scalar Triplet

For completeness we mention that also a Higgs triplet  $\Phi$  belongs to the T-odd sector. The charged Higgs  $\phi^\pm$ , as well as the neutral Higgses  $\phi^0$ ,  $\phi^P$ , are relevant in principle for the decays considered here, but their effects turn out to be of higher order in  $v/f$  as explained in Appendix A. Their mass is given by

$$m_\Phi = \sqrt{2} m_H \frac{f}{v}, \quad (2.10)$$

where  $m_H$  is the mass of the SM Higgs. As pointed out in [24],  $m_H$  in the LHT model can be significantly larger than in supersymmetry.

### 2.4 Weak Mixing in the Mirror Sector

As discussed in detail in [28], one of the important ingredients of the mirror sector is the existence of four CKM-like unitary mixing matrices, two for mirror quarks and two for mirror leptons:

$$V_{Hu}, \quad V_{Hd}, \quad V_{H\ell}, \quad V_{H\nu}. \quad (2.11)$$

They satisfy

$$V_{Hu}^\dagger V_{Hd} = V_{\text{CKM}}, \quad V_{H\nu}^\dagger V_{H\ell} = V_{\text{PMNS}}, \quad (2.12)$$

where in  $V_{\text{PMNS}}$  [44] the Majorana phases are set to zero as the mirror leptons are Dirac particles. The mirror mixing matrices in (2.11) parametrize flavour violating interactions between SM fermions and mirror fermions that are mediated by the heavy gauge bosons  $W_H$ ,  $Z_H$  and  $A_H$ . The notation in (2.11) indicates which of the light fermions of a given electric charge participates in the interaction.

Thus  $V_{Hd}$ , the most important mixing matrix in the present paper, parametrizes the interactions of light  $d^j$ -quarks with heavy mirrors  $u_H^i$  that are mediated by  $W_H$ . It also parametrizes the flavour interactions between  $d^j$  and  $d_H^i$  mediated by  $Z_H$  and  $A_H$ . Feynman rules for these interactions can be found in [28]. We have confirmed those which we needed for the present paper.  $V_{Hu}$ , relevant for  $D^0 - \bar{D}^0$  mixing, parametrizes on the other hand the interactions of the light  $u$ -type quarks with the mirror fermions. Similar comments apply to  $V_{H\nu}$  and  $V_{H\ell}$ .

In the course of our analysis of  $\Delta S = 2$  and  $\Delta B = 2$  processes and in the case of  $B \rightarrow X_s \gamma$  it will be useful to introduce the following quantities ( $i = 1, 2, 3$ ):

$$\xi_i = V_{Hd}^{*is} V_{Hd}^{id}, \quad \xi_i^{(d)} = V_{Hd}^{*ib} V_{Hd}^{id}, \quad \xi_i^{(s)} = V_{Hd}^{*ib} V_{Hd}^{is}, \quad (2.13)$$

that govern  $K^0 - \bar{K}^0$ ,  $B_d^0 - \bar{B}_d^0$  and  $B_s^0 - \bar{B}_s^0$  mixings, respectively.  $\xi_i^{(s)}$  are also relevant for  $B \rightarrow X_s \gamma$ .

Following [28] we will parametrize the matrix  $V_{Hd}$  in the same way as the CKM matrix [45], but with new angles  $\theta_{12}^d$ ,  $\theta_{23}^d$ ,  $\theta_{13}^d$  and the phase  $\delta_{13}^d$ :

$$V_{Hd} = \begin{pmatrix} c_{12}^d c_{13}^d & s_{12}^d c_{13}^d & s_{13}^d e^{-i\delta_{13}^d} \\ -s_{12}^d c_{23}^d - c_{12}^d s_{23}^d s_{13}^d e^{i\delta_{13}^d} & c_{12}^d c_{23}^d - s_{12}^d s_{23}^d s_{13}^d e^{i\delta_{13}^d} & s_{23}^d c_{13}^d \\ s_{12}^d s_{23}^d - c_{12}^d c_{23}^d s_{13}^d e^{i\delta_{13}^d} & -c_{12}^d s_{23}^d - s_{12}^d c_{23}^d s_{13}^d e^{i\delta_{13}^d} & c_{23}^d c_{13}^d \end{pmatrix}. \quad (2.14)$$

The matrix  $V_{Hu}$  is then determined through  $V_{Hu} = V_{Hd} V_{\text{CKM}}^\dagger$ . As in the case of the CKM matrix the angles  $\theta_{ij}^d$  can all be made to lie in the first quadrant with  $0 \leq \delta_{13}^d \leq 2\pi$ .

The matrix  $V_{Hd}$  depends on four parameters that have to be determined in flavour violating processes. In Section 7 we will outline a strategy for this determination. As in the case of the determination of the parameters of the CKM matrix, also here unitarity triangles could play in the future a useful role. On the other hand the structure of the matrix  $V_{Hd}$  can differ in principle by much from the structure of the CKM matrix and using approximations like the Wolfenstein parametrization should be avoided in order to satisfy unitarity exactly.

## 2.5 Mirror Unitarity Triangles

The unitarity of the  $V_{Hd}$  matrix allows to construct six unitarity triangles. The three most important correspond to the unitarity relations

$$\xi_1 + \xi_2 + \xi_3 = 0 \quad (K^0 - \bar{K}^0), \quad (2.15)$$

$$\xi_1^{(d)} + \xi_2^{(d)} + \xi_3^{(d)} = 0 \quad (B_d^0 - \bar{B}_d^0), \quad (2.16)$$

$$\xi_1^{(s)} + \xi_2^{(s)} + \xi_3^{(s)} = 0 \quad (B_s^0 - \bar{B}_s^0). \quad (2.17)$$

In the SM, the hierarchical structure of the elements of the CKM matrix implies rather squashed unitarity triangles in the  $K^0 - \bar{K}^0$  and  $B_s^0 - \bar{B}_s^0$  systems with the famous unitarity triangle in the  $B_d^0 - \bar{B}_d^0$  system, corresponding to

$$V_{ud}V_{ub}^* + V_{cd}V_{cb}^* + V_{td}V_{tb}^* = 0, \quad (2.18)$$

having all sides of the same order of magnitude.

We have clearly no idea at present what the shapes of the mirror unitarity triangles are. The lessons from neutrino physics teach us that they could be very different from the ones encountered in the SM. In Section 7 we will see that in the most interesting scenarios the structure of  $V_{Hd}$  is very different from the CKM one implying significantly different mirror unitarity triangles than the one following from (2.18). We will return to this issue in [36], where our analysis will be generalized to rare  $K$  and  $B$  decays.

## 2.6 The Parameters of the LHT Model

The new parameters in the LHT model, relevant for the present study, are

$$f, \quad x_L, \quad m_{H1}, \quad m_{H2}, \quad m_{H3}, \quad \theta_{12}^d, \quad \theta_{13}^d, \quad \theta_{23}^d, \quad \delta_{13}^d. \quad (2.19)$$

The determination of all these parameters with the help of flavour violating processes is clearly a formidable task. On the other hand once LHC starts its operation and the new particles present in the LHT model are discovered, we will determine  $f$  from  $M_{W_H}$ ,  $M_{Z_H}$  or  $M_{A_H}$  and  $x_L$  from  $m_{T_-}$  or  $m_{T_+}$ . Similarly  $m_{Hi}$  will be measured.

Since the CKM parameters can be determined independently of the LHT contributions from tree level decays during the LHC era, the only remaining free parameters among the ones listed in (2.19) are  $\theta_{ij}^d$  and  $\delta_{13}^d$ . They can be, similarly to the parameters of the CKM matrix, determined in flavour violating processes. In this manner also mirror unitarity triangles will be constructed.

However, in contrast to the CKM parameters, the four parameters of the  $V_{Hd}$  matrix cannot be determined with the help of tree level decays. In fact tree level decays are of no

help here because T-parity forbids the contributions of mirror fermions to these decays at tree level. This is a welcome feature for the determination of the CKM parameters from tree level decays independently of the presence of mirror fermions and T-odd particles, but the determination of the parameters of  $V_{Hd}$  can only be done with the help of loop induced decays, unless decays of mirror fermions to light fermions can be measured one day.

In Section 7 we will indicate how the determination of the matrix  $V_{Hd}$  could be done with the help of the processes considered in the present paper. Generalizations to include rare  $K$  and  $B$  decays in this determination will be presented elsewhere [36].

Clearly as the first five parameters in (2.19) are not known at present, we will only be able to study correlations between all these parameters that are implied by the available data.

### 3 Particle-Antiparticle Mixing and CP Violation

#### 3.1 T-even Sector

The contribution of the T-even sector can be directly extracted from [19]. Including the SM box diagrams the effective Hamiltonian for  $\Delta S = 2$  transitions can be written as follows [19]:

$$[\mathcal{H}_{\text{eff}}(\Delta S = 2)]_{\text{even}} = \frac{G_F^2}{16\pi^2} M_{W_L}^2 [\lambda_c^2 \eta_1 S_c + \lambda_t^2 \eta_2 S_t + 2\lambda_c \lambda_t \eta_3 S_{ct}] (\bar{s}d)_{V-A} (\bar{s}d)_{V-A}, \quad (3.1)$$

where  $\lambda_i = V_{is}^* V_{id}$ . In the case of  $B_d^0 - \bar{B}_d^0$  and  $B_s^0 - \bar{B}_s^0$  mixing the first and the last term can be neglected and one finds ( $q = d, s$ )

$$[\mathcal{H}_{\text{eff}}(\Delta B = 2)]_{\text{even}} = \frac{G_F^2}{16\pi^2} M_{W_L}^2 \lambda_t^{(q)2} \eta_B S_t (\bar{b}q)_{V-A} (\bar{b}q)_{V-A}, \quad (3.2)$$

where  $\lambda_t^{(q)} = V_{tb}^* V_{tq}$ . The factors  $\eta_i$  are QCD corrections to which we will return in Section 3.5.

Writing

$$S_t = S_0(x_t) + \Delta S_t + \Delta S_{TT}, \quad S_c = S_0(x_c) + \Delta S_c, \quad S_{ct} = S_0(x_c, x_t) + \Delta S_{ct}, \quad (3.3)$$

with  $S_0$  being the SM contributions, we find directly from [19]

$$\Delta S_t = -2 \frac{v^2}{f^2} x_L^2 P_1(x_t, x_T), \quad \Delta S_c = 0, \quad \Delta S_{ct} = -\frac{v^2}{f^2} x_L^2 P_2(x_c, x_t, x_T), \quad (3.4)$$

$$\Delta S_{TT} \simeq \frac{v^2}{f^2} \frac{x_L^3}{1-x_L} \frac{x_t}{4}, \quad (3.5)$$

with  $P_1(x_t, x_T)$  and  $P_2(x_c, x_t, x_T)$  calculated in [19] and given for completeness in Appendix B. Here,

$$x_c = \frac{m_c^2}{M_{W_L}^2}, \quad x_t = \frac{m_t^2}{M_{W_L}^2}, \quad x_T = \frac{m_{T_+}^2}{M_{W_L}^2}. \quad (3.6)$$

The contribution of the T-even sector to the off-diagonal element  $M_{12}^K$  in the neutral  $K$ -meson mass matrix is then given as follows

$$(M_{12}^K)_{\text{even}} = \frac{G_F^2}{12\pi^2} F_K^2 \hat{B}_K m_K M_{W_L}^2 \left( \overline{M_{12}^K} \right)_{\text{even}}, \quad (3.7)$$

where

$$\left( \overline{M_{12}^K} \right)_{\text{even}} = \lambda_c^{*2} \eta_1 S_c + \lambda_t^{*2} \eta_2 S_t + 2\lambda_c^* \lambda_t^* \eta_3 S_{ct}, \quad (3.8)$$

and  $\hat{B}_K$  is the well-known non-perturbative factor. Similarly for  $B_d^0 - \bar{B}_d^0$  mixing one has

$$(M_{12}^d)_{\text{even}} = \frac{G_F^2}{12\pi^2} F_{B_d}^2 \hat{B}_{B_d} m_{B_d} M_{W_L}^2 \left( \overline{M_{12}^d} \right)_{\text{even}}, \quad (3.9)$$

where

$$\left( \overline{M_{12}^d} \right)_{\text{even}} = \left( \lambda_t^{(d)*} \right)^2 \eta_B S_t. \quad (3.10)$$

In the case of  $B_s^0 - \bar{B}_s^0$  mixing the amplitude  $(M_{12}^s)_{\text{even}}$  can be obtained from (3.9) and (3.10) by simply replacing  $d$  by  $s$ . It should be emphasized that  $\lambda_i^*$  and not  $\lambda_i$  enter these expressions. Replacing  $\lambda_i^*$  erroneously by  $\lambda_i$  in (3.8) would result for instance in the opposite sign in the CP-violating parameter  $\varepsilon_K$ .

### 3.2 T-odd Sector ( $\Delta S = 2$ )

The effective Hamiltonians summarizing the contributions of the mirror fermions and heavy gauge bosons to  $\Delta F = 2$  transitions have for the first time been presented in [28]. We confirm the expressions for these Hamiltonians given in [28] but our phenomenological analysis of the particle-antiparticle mixing presented in Sections 6 and 7 goes far beyond the one of these authors.

Beginning with  $\Delta S = 2$  transitions, the contributing diagrams are shown in Fig. 1. The diagrams in which the gauge bosons run vertically give the same result and bring in a factor of two. Including the combinatorial factor 1/4 we find (the QCD factor  $\eta_2$  will be explained in Section 3.5)

$$[\mathcal{H}_{\text{eff}}(\Delta S = 2)]_{\text{odd}} = \frac{G_F^2}{64\pi^2} M_{W_L}^2 \frac{v^2}{f^2} \eta_2 \sum_{i,j} \xi_i \xi_j F_H(z_i, z_j) (\bar{s}d)_{V-A} (\bar{s}d)_{V-A}, \quad (3.11)$$

where  $\xi_i$  have been defined in (2.13) and  $F_H(z_i, z_j)$  with

$$z_i = \frac{m_{H_i}^2}{M_{W_H}^2}, \quad z'_i = \frac{m_{H_i}^2}{M_{A_H}^2} = z_i a \quad \text{with } a = \frac{5}{\tan^2 \theta_W} \quad (i = 1, 2, 3), \quad (3.12)$$

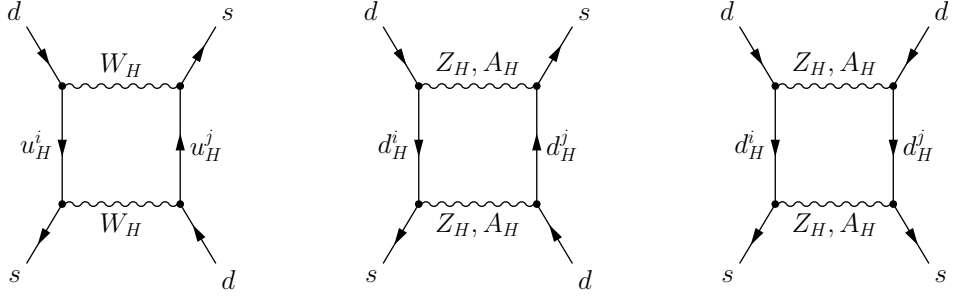


Figure 1: *Diagrams contributing to  $\Delta F = 2$  processes in the T-odd sector.*

are given as follows [28]

$$F_H(z_i, z_j) = F(z_i, z_j; W_H) + G(z_i, z_j; Z_H) + A_1(z_i, z_j; Z_H) + A_2(z_i, z_j; Z_H). \quad (3.13)$$

The different contributions correspond to “WW”, “ZZ”, “AA” and “ZA” diagrams, respectively. Explicit expressions for the functions  $F$ ,  $G$ ,  $A_1$  and  $A_2$  are given in Appendix B.

Using the unitarity relation (2.15) we find then

$$[\mathcal{H}_{\text{eff}}(\Delta S = 2)]_{\text{odd}} = \frac{G_F^2}{64\pi^2} M_{W_L}^2 \frac{v^2}{f^2} \eta_2 [\xi_2^2 R_2(z_1, z_2) + \xi_3^2 R_2(z_1, z_3) + 2\xi_2 \xi_3 R_3(z_1, z_2, z_3)] \cdot (\bar{s}d)_{V-A} (\bar{s}d)_{V-A}, \quad (3.14)$$

where

$$R_2(z_i, z_j) = F_H(z_i, z_i) + F_H(z_j, z_j) - 2F_H(z_i, z_j), \quad (3.15)$$

$$R_3(z_1, z_2, z_3) = F_H(z_2, z_3) + F_H(z_1, z_1) - F_H(z_1, z_2) - F_H(z_1, z_3). \quad (3.16)$$

The contribution of the T-odd sector to the off-diagonal element  $M_{12}^K$  in the neutral  $K$ -meson mass matrix can then be written similarly to (3.7) as follows:

$$(M_{12}^K)_{\text{odd}} = \frac{G_F^2}{48\pi^2} F_K^2 \hat{B}_K m_K M_{W_L}^2 \frac{v^2}{f^2} \eta_2 \left( \overline{M_{12}^K} \right)_{\text{odd}}, \quad (3.17)$$

where

$$\left( \overline{M_{12}^K} \right)_{\text{odd}} = \xi_2^{*2} R_2(z_1, z_2) + \xi_3^{*2} R_2(z_1, z_3) + 2\xi_2^* \xi_3^* R_3(z_1, z_2, z_3). \quad (3.18)$$

### 3.3 T-odd Sector ( $\Delta B = 2$ )

It is straightforward to generalize (3.17) and (3.18) to  $B_d^0 - \bar{B}_d^0$  and  $B_s^0 - \bar{B}_s^0$  mixing. We find for  $B_d^0 - \bar{B}_d^0$  mixing

$$(M_{12}^d)_{\text{odd}} = \frac{G_F^2}{48\pi^2} F_{B_d}^2 \hat{B}_{B_d} m_{B_d} M_{W_L}^2 \frac{v^2}{f^2} \eta_B \left( \overline{M_{12}^d} \right)_{\text{odd}}, \quad (3.19)$$

where

$$\left(\overline{M_{12}^d}\right)_{\text{odd}} = \left(\xi_2^{(d)*}\right)^2 R_2(z_1, z_2) + \left(\xi_3^{(d)*}\right)^2 R_2(z_1, z_3) + 2\xi_2^{(d)*}\xi_3^{(d)*} R_3(z_1, z_2, z_3) \quad (3.20)$$

with  $\xi_i^{(d)}$  defined in (2.13).

Finally in the case of  $B_s^0 - \bar{B}_s^0$  mixing

$$(M_{12}^s)_{\text{odd}} = \frac{G_F^2}{48\pi^2} F_{B_s}^2 \hat{B}_{B_s} m_{B_s} M_{W_L}^2 \frac{v^2}{f^2} \eta_B \left(\overline{M_{12}^s}\right)_{\text{odd}}, \quad (3.21)$$

with  $(\overline{M_{12}^s})_{\text{odd}}$  obtained from  $(\overline{M_{12}^d})_{\text{odd}}$  by replacing  $\xi_i^{(d)}$  by  $\xi_i^{(s)}$ . The QCD factor  $\eta_B$  will be discussed in Section 3.5.

### 3.4 Combining T-odd and T-even Sectors

The final results for  $M_{12}^K$ ,  $M_{12}^d$  and  $M_{12}^s$  in the LHT model that govern the analysis of  $K^0 - \bar{K}^0$ ,  $B_d^0 - \bar{B}_d^0$  and  $B_s^0 - \bar{B}_s^0$  mixing are then

$$M_{12}^i = (M_{12}^i)_{\text{even}} + (M_{12}^i)_{\text{odd}} \quad (i = K, d, s). \quad (3.22)$$

Let us make a few comments:

- The new contributions enter both the even and odd terms. While the even contributions are dominated by the SM part, we will demonstrate in Section 7 that the contributions of the even sector to  $M_{12}^i$  cannot be generally neglected depending on the value of  $x_L$  chosen. Due to electroweak precision constraints only certain combinations of  $x_L$  and  $f$  are allowed [24]. Therefore the contribution of two  $T_+$ , represented by  $\Delta S_{TT}$  in (3.5), can usually be neglected.
- In the limit of exactly degenerate mirror quarks the odd contributions vanish and the LHT model belongs to the class of models with MFV in which all flavour violating processes are governed by the CKM matrix and there are no new operators relative to those present in the SM.<sup>2</sup> As the functions  $P_1$  and  $P_2$  in (3.4) are strictly negative, the new contributions are strictly positive implying generally lower values of  $|V_{td}|$  and  $\gamma$  than coming from the SM fits and an enhanced value of  $\Delta M_s$ , as already pointed out in [19]. The recent measurement of  $\Delta M_s$  suggesting  $\Delta M_s$

<sup>2</sup>Strictly speaking the LHT model in the limit of degenerate mirror quarks belongs to a subclass of MFV models, the so-called Constrained Minimal Flavour Violation (CMFV). In addition to the MFV condition that flavour and CP violation is exclusively governed by the CKM matrix, in CMFV the structure of low energy operators is the same as in the SM. For a detailed discussion on CMFV and MFV we refer to [37].

possibly smaller than  $(\Delta M_s)_{\text{SM}}$  puts therefore an important constraint on the T-even sector unless a rescue comes from the mirror fermions. We will quantify this in Section 7.

- Once the degeneracy of the mirror fermion masses is removed, two new features appear. First a new complex phase  $\delta_{13}^d$ , generally different from  $\delta_{\text{CKM}}$ , enters the game, with profound consequences for  $\varepsilon_K$ ,  $\Delta\Gamma_q$ ,  $A_{\text{SL}}^q$ ,  $A_{\text{CP}}(B_d \rightarrow \psi K_S)$ ,  $A_{\text{CP}}(B_s \rightarrow \psi\phi)$ ,  $A_{\text{CP}}(B \rightarrow X_{s,d}\gamma)$  and also for  $\Delta M_d$  and  $\Delta M_s$  as we will stress below. Equally important, the presence of new mixing angles  $\theta_{ij}^d$ , generally different from  $\theta_{ij}$  in the CKM matrix, introduces new flavour violating interactions leading to the violation of various relations between  $K$ ,  $B_d$ , and  $B_s$  systems that are characteristic for models with MFV [31, 37, 46, 47]. Precisely the violation of these relations could signal the presence of mirror fermion contributions.

### 3.5 QCD Corrections

QCD corrections to  $\Delta F = 2$  transitions in the LH model without T-parity and with T-parity have already been discussed in [19] and [28], respectively. Here we will only summarize the strategy of both papers, that we will follow throughout our analysis, pointing out the difference between the QCD corrections in the T-even and T-odd sectors.

- Below the thresholds of heavy particles, the QCD corrections are at leading order identical to the ones in the SM up to the value of the high energy scale below which only SM particles are present in the effective theory. This is simply related to the fact that at LO only the anomalous dimensions of the involved operators matter [48]. As the operators present in the LHT model are the same as in the SM, the QCD corrections in this approximation can be directly obtained from the SM ones, and the same applies to the non-perturbative parameters  $\hat{B}_i$  that in fact are identical to the ones present in the SM. At NLO, the  $\mathcal{O}(\alpha_s)$  corrections at the matching scale between the full theory with all heavy particles and the effective theory described by the SM will differ from the corresponding matching corrections in the SM. The experience from the calculations of such corrections in supersymmetric theories, however, shows that they are small due to the smallness of  $\alpha_s$  at  $\mu > M_W$  and that they dominantly serve to remove unphysical renormalization scale dependences present at LO. Such a calculation is clearly premature at present and would only be justified after the discovery of mirror fermions, heavy gauge bosons and of  $T_\pm$  heavy quarks.
- It should also be remarked that a proper calculation of QCD corrections would require first the knowledge of the full spectrum of heavy particles involved. In

the case of significant differences between their masses, it could turn out that integrating out all heavy new particles at a single scale, as done in [19, 28] and here, is not a satisfactory approximation and the construction of a sequence of effective theories with a series of thresholds, as done in the SM for scales below  $M_W$ , would be necessary [48]. Clearly such a difficult task is premature at present. However, we would like to emphasize the difference between QCD corrections in the T-even and T-odd sectors.

- In the T-odd sector all particles in the loops are heavy and the structure of the calculation of QCD corrections is similar to the corresponding calculation of the top contributions in the SM. Thus for all contributions from mirror fermions we can use the SM values [49] as seen in (3.17), (3.19) and (3.21)

$$\eta_2 = 0.57 \pm 0.01, \quad \eta_B = 0.55 \pm 0.01. \quad (3.23)$$

- In the T-even sector also light quarks appear in the loops and the calculations of QCD corrections below the scale  $\mathcal{O}(M_W)$  for charm contributions differ from the one for top contributions. In the spirit of the comments made above it is a reasonable approximation to use then in this sector [49]-[51]

$$\eta_1 = 1.32 \pm 0.32, \quad \eta_2 = 0.57 \pm 0.01, \quad \eta_3 = 0.47 \pm 0.05, \quad \eta_B = 0.55 \pm 0.01. \quad (3.24)$$

The contributions of  $T_+$  are absent in the term involving  $\eta_1$  and turn out to be small in the term involving  $\eta_3$ . Consequently  $\eta_1$  and  $\eta_3$  are only relevant for the SM contributions.

### 3.6 Basic Formulae for $\varepsilon_K$ and $\Delta M_i$

In order to study the departures from the SM let us first cast (3.22) into

$$M_{12}^i = (M_{12}^i)_{\text{SM}} + (M_{12}^i)_{\text{new}}, \quad (3.25)$$

with

$$(M_{12}^i)_{\text{new}} = (M_{12}^i)_{\text{even}}^{\text{new}} + (M_{12}^i)_{\text{odd}}, \quad (3.26)$$

$$(M_{12}^i)_{\text{even}}^{\text{new}} = (M_{12}^i)_{\text{even}} - (M_{12}^i)_{\text{SM}}. \quad (3.27)$$

Then the  $K_L - K_S$  mass difference is given by

$$\begin{aligned} \Delta M_K &= 2 [\text{Re} (M_{12}^K)_{\text{SM}} + \text{Re} (M_{12}^K)_{\text{new}}] \\ &= (\Delta M_K)_{\text{SM}} + (\Delta M_K)_{\text{new}}, \end{aligned} \quad (3.28)$$

and  $\varepsilon_K$ , neglecting a small contribution involving  $\text{Re}(M_{12}^K)$ , as follows

$$\begin{aligned}\varepsilon_K &= \frac{e^{i\pi/4}}{\sqrt{2}(\Delta M_K)_{\text{exp}}} [\text{Im}(M_{12}^K)_{\text{SM}} + \text{Im}(M_{12}^K)_{\text{new}}] \\ &= (\varepsilon_K)_{\text{SM}} + (\varepsilon_K)_{\text{new}}.\end{aligned}\quad (3.29)$$

It should be emphasized that there is no interference between the SM and new contributions here. They are simply additive.

We would like to emphasize that this additivity of SM and new contributions is broken in the case of  $\Delta M_d$  and  $\Delta M_s$  if the weak phases of the SM and new contributions differ from each other. Indeed

$$\Delta M_q = 2 |(M_{12}^q)_{\text{SM}} + (M_{12}^q)_{\text{new}}| \quad (q = d, s) \quad (3.30)$$

and the interference between these two contributions can be non-zero and not necessarily constructive. These interferences were not discussed in [28], while they will play an important role in our numerical analysis.

Let us then write

$$(M_{12}^d)_{\text{SM}} \equiv |(M_{12}^d)_{\text{SM}}| e^{2i\varphi_{\text{SM}}^d}, \quad \varphi_{\text{SM}}^d = \beta, \quad (3.31)$$

$$(M_{12}^d)_{\text{new}} \equiv |(M_{12}^d)_{\text{new}}| e^{2i\varphi_{\text{new}}^d}, \quad (3.32)$$

and similarly for  $M_{12}^s$  with  $\varphi_{\text{SM}}^s = \beta_s - \pi$ . Here the phases  $\beta$  and  $\beta_s$  are defined through

$$V_{td} = |V_{td}| e^{-i\beta} \quad \text{and} \quad V_{ts} = -|V_{ts}| e^{-i\beta_s}, \quad (3.33)$$

with  $\beta \simeq 22^\circ$  obtained from UT fits [38, 52] and  $\beta_s \simeq -1^\circ$  from the unitarity of the CKM matrix, its hierarchical structure and its phase conventions. Consequently we can write

$$\Delta M_d = (\Delta M_d)_{\text{SM}} |1 + h_d e^{2i\sigma_d}| \equiv (\Delta M_d)_{\text{SM}} C_{B_d}, \quad (3.34)$$

$$\Delta M_s = (\Delta M_s)_{\text{SM}} |1 + h_s e^{2i\sigma_s}| \equiv (\Delta M_s)_{\text{SM}} C_{B_s}, \quad (3.35)$$

where we have used the model independent notation of [35] and [38, 53], respectively. Here

$$h_i = \left| \frac{(M_{12}^i)_{\text{new}}}{(M_{12}^i)_{\text{SM}}} \right|, \quad \sigma_i = \varphi_{\text{new}}^i - \varphi_{\text{SM}}^i. \quad (3.36)$$

We have then

$$\frac{\Delta M_d}{\Delta M_s} = \frac{m_{B_d}}{m_{B_s}} \frac{\hat{B}_{B_d}}{\hat{B}_{B_s}} \frac{F_{B_d}^2}{F_{B_s}^2} \left| \frac{V_{td}}{V_{ts}} \right|^2 \frac{C_{B_d}}{C_{B_s}}, \quad (3.37)$$

and the MFV relation between  $\Delta M_d/\Delta M_s$  and  $|V_{td}/V_{ts}|^2$  is violated if  $C_{B_d} \neq C_{B_s}$ . We will investigate this violation in Section 7.

### 3.7 $A_{\text{CP}}^{\text{mix}}(B_d \rightarrow \psi K_S)$ and $A_{\text{CP}}^{\text{mix}}(B_s \rightarrow \psi \phi)$

The next to be considered on our list are the mixing induced CP asymmetries in  $B_d^0 \rightarrow \psi K_S$  and  $B_s^0 \rightarrow \psi \phi$  decays, that within the SM and MFV models provide the measurements of the phases  $\beta$  and  $\beta_s$ , respectively, without essentially any theoretical uncertainty. This clean character remains true within the LHT model since

- there are no new tree level contributions to the decay amplitudes for  $B_d^0 \rightarrow \psi K_S$  and  $B_s^0 \rightarrow \psi \phi$  as they are forbidden by T-parity.
- there are no new operators beyond the ones with the  $(V - A) \otimes (V - A)$  structure present in the SM, implying that all non-perturbative uncertainties present in  $M_{12}^i$  will cancel in evaluating the CP asymmetries.

Denoting then as in [35] and [38, 53]

$$1 + h_i e^{2i\sigma_i} = |1 + h_i e^{2i\sigma_i}| e^{2i\varphi_{B_i}} \equiv C_{B_i} e^{2i\varphi_{B_i}}, \quad (3.38)$$

one finds the formulae for the coefficients  $S_{\psi K_S}$  and  $S_{\psi \phi}$  of  $\sin(\Delta M_d t)$  and  $\sin(\Delta M_s t)$ , respectively, in the time dependent asymmetries in question

$$S_{\psi K_S} = -\eta_{\psi K_S} \sin(2\beta + 2\varphi_{B_d}) = \sin(2\beta + 2\varphi_{B_d}), \quad (3.39)$$

$$S_{\psi \phi} = -\eta_{\psi \phi} \sin(2\beta_s + 2\varphi_{B_s}) = \sin(2|\beta_s| - 2\varphi_{B_s}), \quad (3.40)$$

where  $\eta_{\psi K_S}$  and  $\eta_{\psi \phi}$  are the CP parities of the final states. We set  $\eta_{\psi \phi} = +1$ . Thus in the presence of new contributions with  $\sigma_i \neq 0, \pi/2$ , or equivalently  $\varphi_{\text{new}}^i \neq \varphi_{\text{SM}}^i$ ,  $S_{\psi K_S}$  and  $S_{\psi \phi}$  will not measure the phases  $\beta$  and  $\beta_s$  but  $(\beta + \varphi_{B_d})$  and  $(|\beta_s| - \varphi_{B_s})$ , respectively. We will return to investigate this effect numerically in Section 7. Note that it is  $-\varphi_{B_s}$  and not  $+\varphi_{B_s}$  that enters (3.40) [37].

### 3.8 $\Delta\Gamma_q$ and $A_{\text{SL}}^q$

The last quantities we will consider in this section are the width difference  $\Delta\Gamma_q$  and the semileptonic CP asymmetry  $A_{\text{SL}}^q$ , defined respectively as

$$\Delta\Gamma_q = \Gamma_L^q - \Gamma_H^q, \quad (3.41)$$

$$A_{\text{SL}}^q = \frac{\Gamma(\bar{B}_q^0 \rightarrow \ell^+ X) - \Gamma(B_q^0 \rightarrow \ell^- X)}{\Gamma(\bar{B}_q^0 \rightarrow \ell^+ X) + \Gamma(B_q^0 \rightarrow \ell^- X)}, \quad (3.42)$$

with  $q = d, s$  and the light and heavy mass eigenstates given by

$$|B_q^{L,H}\rangle = \frac{1}{\sqrt{1 + |q/p|_q^2}} \left( |B_q^0\rangle \pm \left(\frac{q}{p}\right)_q |\bar{B}_q^0\rangle \right). \quad (3.43)$$

Width difference and semileptonic CP asymmetry are obtained by diagonalizing the  $2 \times 2$  Hamiltonian which describes the  $B_q^0 - \bar{B}_q^0$  systems. Neglecting terms of  $\mathcal{O}(m_b^4/m_t^4)$ , they can simply be written as

$$\Delta\Gamma_q = -\Delta M_q \operatorname{Re} \left( \frac{\Gamma_{12}^q}{M_{12}^q} \right), \quad (3.44)$$

$$A_{\text{SL}}^q = -2 \left( \left| \frac{q}{p} \right|_q - 1 \right) = \operatorname{Im} \left( \frac{\Gamma_{12}^q}{M_{12}^q} \right), \quad (3.45)$$

where  $\Gamma_{12}^q$  is the absorptive part of the  $B_q^0 - \bar{B}_q^0$  amplitude. Theoretical predictions of both  $\Delta\Gamma_q$  and  $A_{\text{SL}}^q$ , therefore, require the calculation of the off-diagonal matrix element  $\Gamma_{12}^q$ .

Important theoretical improvements have been achieved thanks to advances in lattice studies of  $\Delta B = 2$  four-fermion operators [54]-[61] and to the NLO perturbative calculations of the corresponding Wilson coefficients [62]-[65]. From slight updates to the theoretical analysis performed in [62] we find

$$\operatorname{Re} \left( \frac{\Gamma_{12}^d}{M_{12}^d} \right) = -(3.0 \pm 1.0) \cdot 10^{-3}, \quad \operatorname{Re} \left( \frac{\Gamma_{12}^s}{M_{12}^s} \right) = -(2.6 \pm 1.0) \cdot 10^{-3}, \quad (3.46)$$

$$\operatorname{Im} \left( \frac{\Gamma_{12}^d}{M_{12}^d} \right) = -(6.4 \pm 1.4) \cdot 10^{-4}, \quad \operatorname{Im} \left( \frac{\Gamma_{12}^s}{M_{12}^s} \right) = (2.6 \pm 0.5) \cdot 10^{-5}, \quad (3.47)$$

which, combined with the experimental values of lifetimes and mass differences, yield

$$\frac{\Delta\Gamma_d}{\Gamma_d} = (2.3 \pm 0.8) \cdot 10^{-3}, \quad \frac{\Delta\Gamma_s}{\Gamma_s} = (6.7 \pm 2.7) \cdot 10^{-2}, \quad (3.48)$$

$$A_{\text{SL}}^d = -(6.4 \pm 1.4) \cdot 10^{-4}, \quad A_{\text{SL}}^s = (2.6 \pm 0.5) \cdot 10^{-5}. \quad (3.49)$$

We note that the theoretical prediction for  $\operatorname{Re}(\Gamma_{12}^s/M_{12}^s)$  obtained in [62] and updated in (3.46) is smaller than the value found in [63]. This difference is mainly due to the contribution of  $\mathcal{O}(1/m_b^4)$  in the Heavy Quark Expansion (HQE), which in [63] is wholly estimated in the vacuum saturation approximation (VSA), while in [62] the matrix elements of two dimension-seven operators are expressed in terms of those calculated on the lattice. Being the  $\mathcal{O}(1/m_b^4)$  contribution important, it is interesting to estimate the size of the  $\mathcal{O}(1/m_b^5)$  terms. A perturbative calculation of the corresponding Wilson coefficients is now in progress [66].

On the experimental side new relevant measurements exist. The averaged experimental results and limits read [67]

$$\frac{\Delta\Gamma_d}{\Gamma_d} = 0.009 \pm 0.037, \quad \frac{\Delta\Gamma_s}{\Gamma_s} = 0.31^{+0.10}_{-0.11}, \quad (3.50)$$

$$A_{\text{SL}}^d = -(0.0030 \pm 0.0078). \quad (3.51)$$

The comparisons are not yet conclusive, due to still large experimental uncertainties, whose reduction is certainly being looked forward to.

The great interest in confirming or not the SM predictions comes from the sensitivity of these observables to new physics. In the presence of new phases beyond the CKM one, whose effect on  $M_{12}^q$  follows directly from (3.38), one finds

$$\frac{\Delta\Gamma_q}{\Gamma_q} = - \left( \frac{\Delta M_q}{\Gamma_q} \right)^{\text{exp}} \left[ \text{Re} \left( \frac{\Gamma_{12}^q}{M_{12}^q} \right)^{\text{SM}} \frac{\cos 2\varphi_{B_q}}{C_{B_q}} - \text{Im} \left( \frac{\Gamma_{12}^q}{M_{12}^q} \right)^{\text{SM}} \frac{\sin 2\varphi_{B_q}}{C_{B_q}} \right], \quad (3.52)$$

$$A_{\text{SL}}^q = \text{Im} \left( \frac{\Gamma_{12}^q}{M_{12}^q} \right)^{\text{SM}} \frac{\cos 2\varphi_{B_q}}{C_{B_q}} - \text{Re} \left( \frac{\Gamma_{12}^q}{M_{12}^q} \right)^{\text{SM}} \frac{\sin 2\varphi_{B_q}}{C_{B_q}}. \quad (3.53)$$

It is important to note that with  $\text{Re}(\Gamma_{12}^s/M_{12}^s) \gg \text{Im}(\Gamma_{12}^s/M_{12}^s)$ , even a small  $\varphi_{B_s}$  can induce an order of magnitude enhancement of  $A_{\text{SL}}^s$  relative to the SM. On the other hand, a non-vanishing  $\varphi_{B_q}$  would result in a suppression of  $\Delta\Gamma_q/\Gamma_q$ , thus increasing the discrepancy with the experimental average in the  $q = s$  case. We note, however, that the new preliminary experimental average  $\Delta\Gamma_s/\Gamma_s = 0.14 \pm 0.06$  [68] is lower than the previous one, thus reducing significantly the discrepancy with the SM theoretical prediction in (3.48). These topics have been extensively discussed in the recent literature [37, 38, 39, 42]. In [39] a correlation between  $A_{\text{SL}}^s$  and  $S_{\psi\phi}$  has been pointed out and in [37] some correlations have been derived in order to determine the ratio  $\Delta M_q/(\Delta M_q)_{\text{SM}}$  in a theoretically clean way. They read

$$\frac{\Delta M_q}{(\Delta M_q)_{\text{SM}}} = \left| \text{Re} \left( \frac{\Gamma_{12}^q}{M_{12}^q} \right)^{\text{SM}} \right| \frac{\sin 2\varphi_{B_q}}{A_{\text{SL}}^q} + \text{Im} \left( \frac{\Gamma_{12}^q}{M_{12}^q} \right)^{\text{SM}} \frac{\cos 2\varphi_{B_q}}{A_{\text{SL}}^q}, \quad (3.54)$$

$$\frac{\Delta M_q}{(\Delta M_q)_{\text{SM}}} = - \left( \frac{\Delta M_q}{\Delta\Gamma_q} \right) \text{Re} \left( \frac{\Gamma_{12}^q}{M_{12}^q} \right)^{\text{SM}} \cos 2\varphi_{B_q}, \quad (3.55)$$

with  $\varphi_{B_q}$  to be extracted from  $S_{\psi\phi}$  and  $S_{\psi K_S}$  for  $q = s$  and  $q = d$ , respectively. In the case of  $q = s$ , the second term in (3.54) can be safely neglected. It will be interesting to consider these correlations within the LHT model once the experimental uncertainties have been significantly reduced.

### 3.9 Summary

In this section we have calculated the  $\mathcal{O}(v^2/f^2)$  corrections to the amplitudes  $M_{12}^K$ ,  $M_{12}^d$  and  $M_{12}^s$  in the LHT model confirming the results of [28]. We have then given formulae for  $\Delta M_K$ ,  $\Delta M_d$ ,  $\Delta M_s$ ,  $\varepsilon_K$ ,  $S_{\psi K_S}$ ,  $S_{\psi\phi}$ ,  $\Delta\Gamma_q$  and  $A_{\text{SL}}^q$  in a form suitable for the study of the size of the new LHT contribution. The numerical analysis of these observables will be presented in Section 7.

## 4 $B \rightarrow X_s \gamma$ in the LHT Model

### 4.1 Preliminaries

One of the most popular decays used to constrain new physics contributions is the  $B \rightarrow X_s \gamma$  decay for which the measured branching ratio [67]

$$Br(B \rightarrow X_s \gamma)_{\text{exp}} = (3.52 \pm 0.30) \cdot 10^{-4} \quad (4.1)$$

agrees well with the SM NLO prediction [69, 70]

$$Br(B \rightarrow X_s \gamma)_{\text{SM}} = (3.33 \pm 0.29) \cdot 10^{-4}, \quad (4.2)$$

both given for  $E_\gamma > 1.6$  GeV and the SM prediction for  $m_c(m_c)/m_b^{1S} = 0.26$ . For  $Br(B \rightarrow X_d \gamma)$ , instead, the SM prediction is in the ballpark of  $1.5 \cdot 10^{-5}$ .

One should emphasize that within the SM this decay is governed by the already well determined CKM element  $|V_{ts}|$  so that dominant uncertainties in (4.2) result from the truncation of the QCD perturbative series and the value of  $m_c(\mu)$  that enters the branching ratio first at the NLO level. A very difficult NNLO calculation, presently in progress [70], should reduce the error in (4.2) below 10%.

The effective Hamiltonian relevant for this decay within the SM is given as follows

$$\mathcal{H}_{\text{eff}}^{\text{SM}}(\bar{b} \rightarrow \bar{s} \gamma) = -\frac{G_F}{\sqrt{2}} V_{ts} V_{tb}^* \left[ \sum_{i=1}^6 C_i(\mu_b) Q_i + C_{7\gamma}(\mu_b) Q_{7\gamma} + C_{8G}(\mu_b) Q_{8G} \right], \quad (4.3)$$

where  $Q_i$  are four-quark operators,  $Q_{7\gamma}$  is the magnetic photon penguin operator and  $Q_{8G}$  the magnetic gluon penguin operator. The explicit expression for the branching ratio  $Br(B \rightarrow X_s \gamma)$  resulting from (4.3) is very complicated and we will not present it here. It can be found for instance in [69].

For our purposes it is sufficient to know that in the LO approximation the Wilson coefficients  $C_{7\gamma}$  and  $C_{8G}$  are given at the renormalization scale  $\mu_W = \mathcal{O}(M_W)$  as follows

$$C_{7\gamma}^0(\mu_W) = -\frac{1}{2} D'_0(x_t), \quad C_{8G}^0(\mu_W) = -\frac{1}{2} E'_0(x_t), \quad (4.4)$$

with the explicit expressions for  $D'_0(x_t)$  and  $E'_0(x_t)$  given in Appendix B.

In view of the importance of QCD corrections in this decay we will include these corrections at NLO in the SM part, but only at LO in the new contributions. This amounts to including only corrections to the renormalization of the operators in the LHT part and eventually to increase the scale  $\mu_W$  to  $\mu \approx 500$  GeV at which the new particles are integrated out. As the dominant QCD corrections to  $Br(B \rightarrow X_s \gamma)$  come anyway from the renormalization group evolution from  $\mu_W$  down to  $\mu_b = \mathcal{O}(m_b)$  and

the matrix elements of the operators  $Q_2$  and  $Q_{7\gamma}$  at  $\mu_b$ , these dominant corrections are common to the SM and LHT parts.

Within the LO approximation the new physics contributions to  $B \rightarrow X_s\gamma$  enter only through the modifications of the following two combinations

$$T_{D'}^{\text{SM}} \equiv \lambda_t^{(s)} D'_0(x_t), \quad T_{E'}^{\text{SM}} \equiv \lambda_t^{(s)} E'_0(x_t), \quad (4.5)$$

with the CKM factor  $\lambda_t^{(s)} = V_{ts} V_{tb}^*$ .

## 4.2 T-even Sector

The first calculation of the  $B \rightarrow X_s\gamma$  decay within the LH model has been done within the Littlest Higgs model without T-parity in [22]. We have confirmed this result. Specializing it to the LHT model leaves at  $\mathcal{O}(v^2/f^2)$  only the contributions shown in Fig. 2. The result can be directly obtained by changing the arguments in  $D'_0(x_t)$  and  $E'_0(x_t)$ . We find then

$$T_{D'}^{\text{even}} = \lambda_t^{(s)} \left[ D'_0(x_t) + \frac{v^2}{f^2} x_L^2 (D'_0(x_T) - D'_0(x_t)) \right], \quad (4.6)$$

$$T_{E'}^{\text{even}} = \lambda_t^{(s)} \left[ E'_0(x_t) + \frac{v^2}{f^2} x_L^2 (E'_0(x_T) - E'_0(x_t)) \right], \quad (4.7)$$

with  $x_t$  and  $x_T$  defined in (3.6).

The calculation for the  $B \rightarrow X_d\gamma$  decay is completely analogous and the corresponding T-even contributions can be obtained from (4.6) and (4.7) with the replacement  $s \rightarrow d$ .

## 4.3 T-odd Sector

The diagrams contributing at  $\mathcal{O}(v^2/f^2)$  in this sector are shown in Fig. 3. The results for these diagrams can be easily obtained from  $D'_0(x_t)$  and  $E'_0(x_t)$  as follows. The contributions from  $W_H^\pm$  can be found directly as in the even sector. The contributions of  $A_H$  and  $Z_H$  can be on the other hand obtained from  $E'_0(x_t)$  as, similarly to the gluon penguin, they do not contain triple weak gauge boson vertices.

We find first using the unitarity of the  $V_{H_d}$  matrix

$$T_{D'}^{\text{odd}} = \frac{1}{4} \frac{v^2}{f^2} \left[ \xi_2^{(s)} (D'_{\text{odd}}(z_2) - D'_{\text{odd}}(z_1)) + \xi_3^{(s)} (D'_{\text{odd}}(z_3) - D'_{\text{odd}}(z_1)) \right], \quad (4.8)$$

$$T_{E'}^{\text{odd}} = \frac{1}{4} \frac{v^2}{f^2} \left[ \xi_2^{(s)} (E'_{\text{odd}}(z_2) - E'_{\text{odd}}(z_1)) + \xi_3^{(s)} (E'_{\text{odd}}(z_3) - E'_{\text{odd}}(z_1)) \right]. \quad (4.9)$$

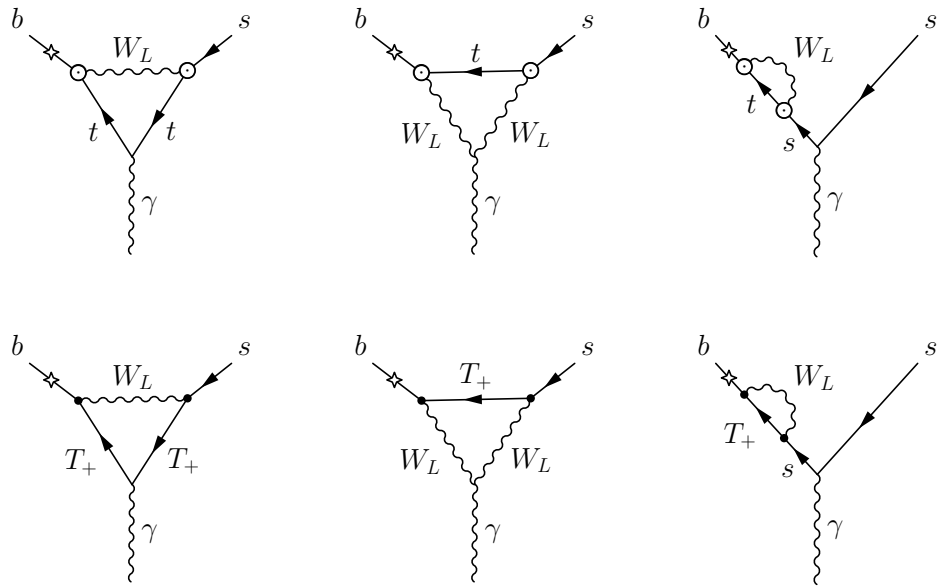


Figure 2: *New diagrams contributing to  $B \rightarrow X_s \gamma$  in the T-even sector.*

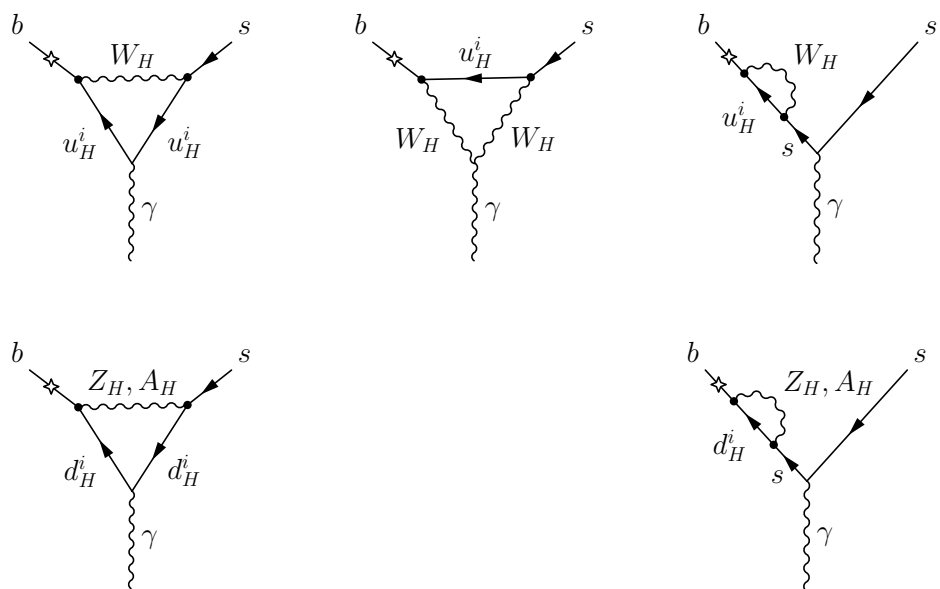


Figure 3: *Diagrams contributing to  $B \rightarrow X_s \gamma$  in the T-odd sector.*

A straightforward calculation gives then

$$D'_{\text{odd}}(z_i) = D'_0(z_i) - \frac{1}{6}E'_0(z_i) - \frac{1}{30}E'_0(z'_i), \quad (4.10)$$

$$E'_{\text{odd}}(z_i) = E'_0(z_i) + \frac{1}{2}E'_0(z_i) + \frac{1}{10}E'_0(z'_i), \quad (4.11)$$

where the three contributions correspond to  $W_H$ ,  $Z_H$  and  $A_H$  exchanges, respectively. The variables  $z_i$  and  $z'_i$  are defined in (3.12).

Similarly to the T-even sector, the T-odd contributions to the  $B \rightarrow X_d\gamma$  decay can be obtained in a trivial way, with the replacement  $s \rightarrow d$  in (4.8) and (4.9).

#### 4.4 CP Asymmetry in $B \rightarrow X_{s,d}\gamma$

In view of the new weak phase present in the LHT model, of particular interest is the direct CP asymmetry in  $B \rightarrow X_s\gamma$  that due to a very small phase of  $V_{ts}$  is about 0.5% in the SM. In the case of  $B \rightarrow X_d\gamma$ , the corresponding asymmetry is governed in the SM by the phase  $\gamma + \beta$  and is about  $-10\%$ . Consequently, it will be harder to see new physics in this case unless the experiment shows an opposite sign. Defining

$$C_{7\gamma}(m_b) = -|C_{7\gamma}(m_b)|e^{i\phi_7}, \quad C_{8G}(m_b) = -|C_{8G}(m_b)|e^{i\phi_8}, \quad (4.12)$$

and using the formulae of [71] it is straightforward to calculate the CP asymmetries in question. We recall that in the SM  $\phi_7 = \phi_8 = 0$ .

#### 4.5 Summary

In this section we have calculated, for the first time, the  $\mathcal{O}(v^2/f^2)$  corrections to the  $B \rightarrow X_s\gamma$  decay in the LHT model. The final results can be summarized by

$$T_{D'} = T_{D'}^{\text{even}} + T_{D'}^{\text{odd}}, \quad T_{E'} = T_{E'}^{\text{even}} + T_{E'}^{\text{odd}}, \quad (4.13)$$

with the various terms given in (4.6)–(4.9). The numerical analysis of the branching ratios and the CP asymmetries in question will be given in Section 7.

Our result for  $T_{E'}$  can also be used for the  $b \rightarrow s g$  decay, but in view of very large theoretical uncertainties in the corresponding branching ratio we will not consider it here.

## 5 Strategy and Goals

In what follows it will be useful to recall the unitarity triangle shown in Fig. 4 with  $R_b$  and  $R_t$  given as follows

$$R_b = \frac{|V_{ud}V_{ub}^*|}{|V_{cd}V_{cb}^*|}, \quad R_t = \frac{|V_{td}V_{tb}^*|}{|V_{cd}V_{cb}^*|}. \quad (5.1)$$

Using  $R_b$  and  $\gamma$  determined in tree level decays one can construct the so-called reference unitarity triangle (RUT) [72] with  $R_b$  and  $\gamma$  independent of new physics contributions and denoted therefore by  $(R_b)_{\text{true}}$  and  $\gamma_{\text{true}}$ . On the other hand using the MFV relations [37]

$$\sin 2\beta = S_{\psi K_S} \equiv \sin 2\beta_{\text{MFV}}, \quad (5.2)$$

$$R_t = 0.923 \left[ \frac{\xi}{1.23} \right] \sqrt{\frac{17.4/\text{ps}}{\Delta M_s}} \sqrt{\frac{\Delta M_d}{0.507/\text{ps}}} \equiv (R_t)_{\text{MFV}}, \quad (5.3)$$

where [73]

$$\xi = \frac{\sqrt{\hat{B}_{B_s} F_{B_s}}}{\sqrt{\hat{B}_{B_d} F_{B_d}}} = 1.23 \pm 0.06, \quad (5.4)$$

allows to construct the UUT [31]. The two triangles are related through

$$R_b = \sqrt{1 + R_t^2 - 2R_t \cos \beta}, \quad \cot \gamma = \frac{1 - R_t \cos \beta}{R_t \sin \beta}, \quad (5.5)$$

and the violation of these relations would in the context of the LHT model signal the presence of new flavour and CP-violating interactions. Indeed the low energy operator structure in the LHT model is the same as in the SM and rescue from new operators cannot be expected.

A detailed test of the relations in (5.5) is presently not possible in view of sizable theoretical and experimental uncertainties and the fact that the two triangles do not differ by much from each other as seen in Fig. 4. Yet, if one desperately looks for some differences between these two triangles one finds that the “true” values of various parameters extracted from the RUT differ from the corresponding MFV values [37, 38, 74, 75]

$$\beta_{\text{true}} > \beta_{\text{MFV}}, \quad \gamma_{\text{true}} > \gamma_{\text{MFV}}, \quad (R_t)_{\text{true}} > (R_t)_{\text{MFV}}, \quad (R_b)_{\text{true}} > (R_b)_{\text{MFV}}. \quad (5.6)$$

In particular, there is a tension between the MFV value of  $\sin 2\beta$  and the one indicated by the true value of  $R_b$ , as discussed in detail in [37].

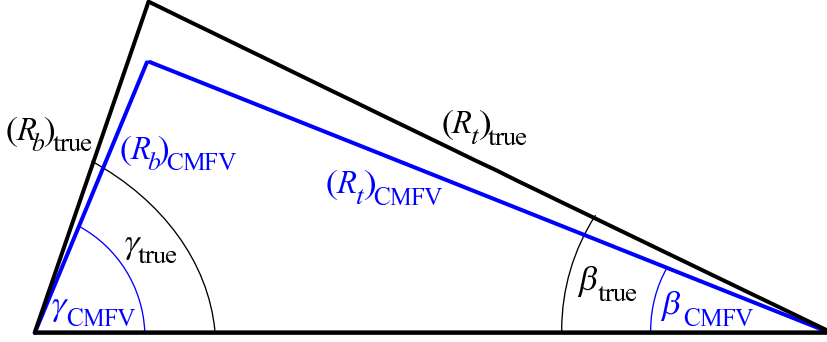


Figure 4: *Reference unitarity triangle and universal unitarity triangle* [37].

Moreover, the measured value of  $\Delta M_s$  [29]

$$\Delta M_s = (17.33^{+0.42}_{-0.21} \pm 0.07) / \text{ps} \quad (5.7)$$

turned out to be surprisingly below the SM predictions obtained from other constraints [38, 52]

$$(\Delta M_s)_{\text{UTfit}}^{\text{SM}} = (21.5 \pm 2.6) / \text{ps}, \quad (\Delta M_s)_{\text{CKMfitter}}^{\text{SM}} = (21.7^{+5.9}_{-4.2}) / \text{ps}. \quad (5.8)$$

The slight tension between (5.7) and (5.8) is not yet significant as the non-perturbative uncertainties are large but it appears that

$$\Delta M_s < (\Delta M_s)_{\text{SM}} \quad (5.9)$$

could be favoured.

Our three goals for the next two Sections are then as follows:

1. We will consider the MFV limit of the LHT model in which the problems in (5.6) and (5.9) cannot be solved.
2. We will investigate whether the problems listed in (5.6) and (5.9) can be solved within the LHT model with the help of new flavour and CP-violating interactions encoded in the matrix  $V_{Hd}$  by choosing a special pattern of the mirror fermion mass spectrum.

Once new CP-violating phases are present, the CP asymmetries  $A_{\text{CP}}(B_s \rightarrow \psi\phi)$ ,  $A_{\text{SL}}^q$  and  $A_{\text{CP}}(B \rightarrow X_s\gamma)$  can be significantly larger than in the SM. This brings us to our third goal:

3. We will look for interesting benchmark scenarios for the matrix  $V_{Hd}$  and for the mass spectrum of mirror fermions in which large enhancements of  $A_{\text{CP}}(B_s \rightarrow \psi\phi)$ ,  $A_{\text{SL}}^q$  and  $A_{\text{CP}}(B \rightarrow X_s\gamma)$  over the SM values are possible being still consistent with all other constraints. We will also investigate the implications for  $\Delta\Gamma_q/\Gamma_q$ .

## 6 Benchmark Scenarios for New Parameters

### 6.1 Preliminaries

In what follows we will consider several scenarios for the structure of the  $V_{Hd}$  matrix and the mass spectrum of mirror fermions with the hope to gain a global view about the possible signatures of mirror fermions in the processes considered and of  $T_+$  present in the T-even contributions.

The most interesting scenarios in the model in question will be those in which the mixing matrix  $V_{Hd}$  differs significantly from  $V_{CKM}$  and has a non-vanishing complex phase  $\delta_{13}^d$ . As now the number of parameters increases significantly, it is essential to determine the CKM parameters from tree level decays. The left-over room for new physics contributions will depend on the outcome of this determination.

Now for given values of  $|V_{ub}|$ ,  $|V_{cb}|$  and  $|V_{us}|$  and the angle  $\gamma$  in the CKM unitarity triangle, the true phases of the  $V_{td}$  and  $V_{ts}$  couplings are determined and the asymmetries  $S_{\psi K_s}$  and  $S_{\psi \phi}$  in (3.39) and (3.40), respectively, can be predicted by setting first  $\varphi_{B_d}$  and  $\varphi_{B_s}$  to zero. Similarly,  $\varepsilon_K$ ,  $\Delta M_K$ ,  $\Delta M_d$ ,  $\Delta M_s$  and  $Br(B \rightarrow X_s \gamma)$  can be predicted and compared with the experiments, possibly revealing the need for new physics contributions, as discussed in previous sections.

In the next section we will be primarily interested in achieving the three goals listed in Section 5. Moreover, it will be interesting to see how the MFV correlations between  $K^0$ ,  $B_d^0$  and  $B_s^0$  systems are modified when new sources of flavour and CP violation are present. Effectively, such modifications can be studied by introducing effective one-loop functions  $(S_i)_{\text{eff}}$

$$(S_i)_{\text{eff}} = S_0(x_t) C_i e^{2i\varphi_i}, \quad i = K, B_d, B_s \quad (6.1)$$

with  $C_i$  and  $\varphi_i$  already defined in (3.38). In MFV

$$C_K = C_{B_d} = C_{B_s}, \quad \varphi_K = \varphi_{B_d} = \varphi_{B_s} = 0, \quad (6.2)$$

but as we will see below, this is generally not the case in the LHT model. In particular we will investigate the violation of the MFV relation between  $\Delta M_d/\Delta M_s$  and  $|V_{td}/V_{ts}|$  obtained for  $C_{B_d} = C_{B_s}$  in (3.37).

It is not a purpose of our numerical analysis of the next section to consider the full space of parameters but rather to have a closer look at a number of scenarios in which some of the problems listed above can be simply addressed. Not all the scenarios listed below solve the problems in question and some of them give results that are very close to the SM predictions, but we found at least one scenario (S4) in which all our goals have been achieved. In this scenario, the  $V_{Hd}$  matrix takes a hierarchical structure that is very different from the structure of the CKM matrix.

## 6.2 Different Scenarios

Here we just list the scenarios in question:

### Scenario 1:

In this scenario the mirror fermions will be degenerate in mass

$$m_{H1} = m_{H2} = m_{H3} \quad (6.3)$$

and only the T-even sector will contribute. This is the MFV limit of the LHT model.

### Scenario 2:

In this scenario the mirror fermions are not degenerate in mass and

$$V_{Hd} = V_{\text{CKM}}. \quad (6.4)$$

In this case there are no contributions of mirror fermions to  $D^0 - \bar{D}^0$  mixing and flavour violating  $D$  meson decays, and

$$\xi_2^{(q)} = \lambda_c^{(q)}, \quad \xi_3^{(q)} = \lambda_t^{(q)}, \quad (6.5)$$

with  $q = d, s$  and no index  $q$  in the  $K$  system.

### Scenario 3:

In this scenario we will choose a linear spectrum for mirror fermions

$$m_{H1} = 400 \text{ GeV}, \quad m_{H2} = 500 \text{ GeV}, \quad m_{H3} = 600 \text{ GeV} \quad (6.6)$$

but an otherwise arbitrary matrix  $V_{Hd}$ . We stress that similar results are obtained by changing the values above by  $\pm 30$  GeV, with similar comments applying to (6.7) and (6.12) below.

### Scenario 4:

This is our favourite scenario in which the most interesting departures from the SM and MFV can be obtained and the problems addressed by us before can be solved. In this scenario

$$m_{H1} \approx m_{H2} = 500 \text{ GeV}, \quad m_{H3} = 1000 \text{ GeV}, \quad (6.7)$$

$$\frac{1}{\sqrt{2}} \leq s_{12}^d \leq 0.99, \quad 5 \cdot 10^{-5} \leq s_{23}^d \leq 2 \cdot 10^{-4}, \quad 4 \cdot 10^{-2} \leq s_{13}^d \leq 0.6 \quad (6.8)$$

and the phase  $\delta_{13}^d$  is arbitrary. The hierarchical structure of the CKM matrix

$$s_{13} \ll s_{23} \ll s_{12}, \quad (\text{CKM}) \quad (6.9)$$

is changed in this scenario to

$$s_{23}^d \ll s_{13}^d \leq s_{12}^d, \quad (V_{Hd}) \quad (6.10)$$

so that  $V_{Hd}$  looks as follows:

$$V_{Hd} = \begin{pmatrix} c_{12}^d & s_{12}^d & s_{13}^d e^{-i\delta_{13}^d} \\ -s_{12}^d & c_{12}^d & s_{23}^d \\ -c_{12}^d s_{13}^d e^{i\delta_{13}^d} & -s_{12}^d s_{13}^d e^{i\delta_{13}^d} & 1 \end{pmatrix}. \quad (6.11)$$

The very different structure of  $V_{Hd}$  when compared with  $V_{CKM}$ , with a large complex phase in the  $(V_{Hd})_{32}$  element assures large CP-violating effects in the  $B_s^0 - \bar{B}_s^0$  system without any problem with  $\Delta M_K$  as the first two mirror fermion masses are very close to each other. Furthermore  $\Delta M_s$  can be smaller than its SM value in this scenario, and interesting effects in the  $B_d^0 - \bar{B}_d^0$  system are also found.

### Scenario 5:

In all the previous scenarios we will choose the first solution for the angle  $\gamma$  from tree level decays as given in (7.1) below so that only small departures from the SM in the  $B_d^0 - \bar{B}_d^0$  system will be consistent with the data. Here we will assume the second solution for  $\gamma$  in (7.1) in contradiction with the SM and MFV. We will then ask whether the presence of new flavour violating interactions can still bring the theory to agree with all available data, in particular with the asymmetry  $S_{\psi K_S}$ .

It turns out that for a particular choice of the parameters of the LHT model, consistency with all existing data can be obtained, although this scenario appears to be less likely than Scenario 4.

In this scenario

$$m_{H1} = 500 \text{ GeV}, \quad m_{H2} = 450 \text{ GeV}, \quad m_{H3} = 1000 \text{ GeV}, \quad (6.12)$$

$$5 \cdot 10^{-5} \leq s_{12}^d \leq 0.015, \quad 2 \cdot 10^{-2} \leq s_{23}^d \leq 4 \cdot 10^{-2}, \quad 0.2 \leq s_{13}^d \leq 0.5 \quad (6.13)$$

and the phase  $\delta_{13}^d$  arbitrary. We thus have an inverted hierarchy relative to the CKM one in (6.9) but also different from the one in scenario 4:

$$s_{12}^d \leq s_{23}^d \ll s_{13}^d, \quad (V_{Hd}). \quad (6.14)$$

$V_{Hd}$  looks now as follows:

$$V_{Hd} = \begin{pmatrix} c_{13}^d & s_{12}^d c_{13}^d & s_{13}^d e^{-i\delta_{13}^d} \\ -s_{12}^d & c_{12}^d & s_{23}^d c_{13}^d \\ -s_{13}^d e^{i\delta_{13}^d} & -s_{23}^d & c_{13}^d \end{pmatrix} \approx \begin{pmatrix} c_{13}^d & 0 & s_{13}^d e^{-i\delta_{13}^d} \\ 0 & 1 & 0 \\ -s_{13}^d e^{i\delta_{13}^d} & 0 & c_{13}^d \end{pmatrix}. \quad (6.15)$$

The very different structure of  $V_{Hd}$  when compared with  $V_{CKM}$ , allows to make this scenario compatible with the data. The price one has to pay are tiny new physics effects in the  $B_s^0 - \bar{B}_s^0$  system.

## 7 Numerical Analysis

### 7.1 Preliminaries

In our numerical analysis we will set  $|V_{us}|$ ,  $|V_{cb}|$  and  $|V_{ub}|$  to their central values measured in tree level decays [67, 76] and collected in Table 1.

$G_F = 1.16637 \cdot 10^{-5} \text{ GeV}^{-2}$	$\Delta M_K = 3.483(6) \cdot 10^{-15} \text{ GeV}$
$M_W = 80.425(38) \text{ GeV}$	$\Delta M_d = 0.507(4) \text{ ps}$ [67]
$\alpha = 1/127.9$	$\Delta M_s = 17.4(4) \text{ ps}$ [29, 30]
$\sin^2 \theta_W = 0.23120(15)$ [77]	$F_K \sqrt{\hat{B}_K} = 143(7) \text{ MeV}$ [73, 77]
$ V_{ub}  = 0.00423(35)$	$F_D \sqrt{\hat{B}_D} = 202(39) \text{ MeV}$ [78]
$ V_{cb}  = 0.0416(7)$ [67]	$F_{B_d} \sqrt{\hat{B}_{B_d}} = 214(38) \text{ MeV}$
$\lambda =  V_{us}  = 0.225(1)$ [76]	$F_{B_s} \sqrt{\hat{B}_{B_s}} = 262(35) \text{ MeV}$ [73]
$ V_{ts}  = 0.0409(9)$ [38]	$\eta_1 = 1.32(32)$ [50]
$m_{K^0} = 497.65(2) \text{ MeV}$	$\eta_3 = 0.47(5)$ [51]
$m_{D^0} = 1.8645(4) \text{ GeV}$	$\eta_2 = 0.57(1)$
$m_{B_d} = 5.2794(5) \text{ GeV}$	$\eta_B = 0.55(1)$ [49]
$m_{B_s} = 5.370(2) \text{ GeV}$	$\bar{m}_c = 1.30(5) \text{ GeV}$
$ \varepsilon_K  = 2.284(14) \cdot 10^{-3}$ [77]	$\bar{m}_t = 163.8(32) \text{ GeV}$
$S_{\psi K_S} = 0.687(32)$ [67]	

Table 1: *Values of the experimental and theoretical quantities used as input parameters.*

As the fourth parameter we will choose the angle  $\gamma$  in the standard UT that to an excellent approximation equals the phase  $\delta_{\text{CKM}}$  in the CKM matrix. The angle  $\gamma$  has been extracted from  $B \rightarrow D^{(*)}K$  decays without the influence of new physics with the result [38]

$$\gamma = (71 \pm 16)^\circ, \quad \gamma = -(109 \pm 16)^\circ. \quad (7.1)$$

Only the first solution agrees with the SM analysis of the UT but as we go beyond the SM in the present paper we will investigate in Scenario 5 whether the second solution could be consistent with the data within the LHT model. The error in the first solution is sufficiently large to allow for significant contributions from new physics.

For the non-perturbative parameters entering the analysis of particle-antiparticle mixing we choose and collect in Table 1 their lattice averages given in [73], which combine unquenched results obtained with different lattice actions.

In order to simplify our numerical analysis we will set all non-perturbative parameters to their central values and instead we will allow  $\Delta M_K$ ,  $\varepsilon_K$ ,  $\Delta M_d$ ,  $\Delta M_s$  and  $S_{\psi K_S}$  to differ from their experimental values by  $\pm 50\%$ ,  $\pm 30\%$ ,  $\pm 40\%$ ,  $\pm 40\%$  and  $\pm 8\%$ , respectively.

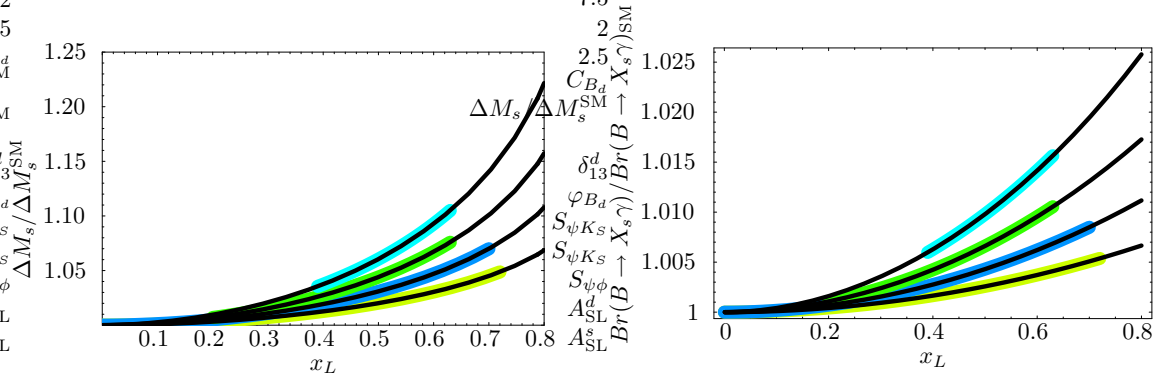


Figure 5:  $\Delta M_s / (\Delta M_s)_{SM}$  and  $Br(B \rightarrow X_s\gamma) / Br(B \rightarrow X_s\gamma)_{SM}$  in Scenario 1 as functions of  $x_L$  for values of  $f = 1, 1.2, 1.5$ , and  $2$  TeV from top to bottom. The bands underlying the curves show the allowed ranges after applying electroweak precision constraints [24].

This could appear rather conservative, but we do not want to miss any interesting effects by choosing too optimistic non-perturbative uncertainties. In Scenarios 3 – 5, then, the parameters  $f$  and  $x_L$  will be fixed to  $f = 1000$  GeV and  $x_L = 0.5$  in accordance with electroweak precision tests [24].

## 7.2 Scenario 1

Let us consider first the case of totally degenerate mirror fermions. In this case the odd contributions vanish due to the GIM mechanism [79], the only new particle contributing is  $T_+$  and the LHT model in this limit belongs to the class of MFV models. As only the T-even sector contributes, the new contributions to particle-antiparticle mixing and  $B \rightarrow X_s\gamma$  are entirely dependent on only two parameters

$$x_L, \quad f. \quad (7.2)$$

Moreover, all the dependence on new physics contributions is encoded in the function  $S_t$  in (3.3) in the case of particle-antiparticle mixing and the functions  $T_{D'}^{\text{even}}$  and  $T_{E'}^{\text{even}}$  in (4.6) and (4.7) in the case of the  $B \rightarrow X_s\gamma$  decay.

It should be emphasized that in this scenario the “problems” listed in (5.6) cannot be solved as it is a MFV scenario. Moreover,  $\Delta M_s \geq (\Delta M_s)_{SM}$ , which is not favoured by the CDF measurement. Also  $\Delta M_d \geq (\Delta M_d)_{SM}$  in this scenario. Therefore in Fig. 5 we show the ratio  $\Delta M_s / (\Delta M_s)_{SM}$  and the corresponding ratio for  $Br(B \rightarrow X_s\gamma)$  as functions of  $x_L$  for various values of  $f$ .

We find that the maximal relative enhancements with respect to the SM are 10% for  $\Delta M_s$  and about 1.5% for  $Br(B \rightarrow X_s\gamma)$ . In view of large theoretical errors in the

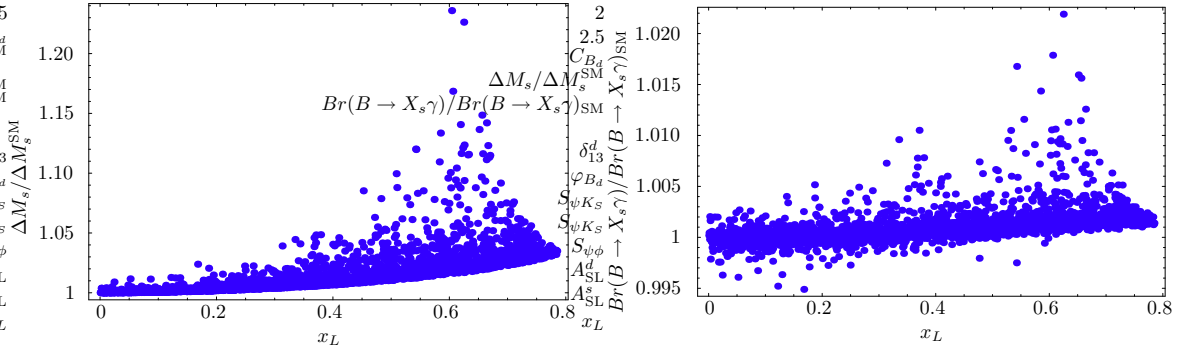


Figure 6:  $\Delta M_s / (\Delta M_s)^{\text{SM}}$  and  $\text{Br}(B \rightarrow X_s \gamma) / \text{Br}(B \rightarrow X_s \gamma)^{\text{SM}}$  as functions of  $x_L$  in Scenario 2.

evaluation of  $\Delta M_{d,s}$ , however, this scenario cannot be tested at present. Similarly to  $\text{Br}(B \rightarrow X_s \gamma)$ , the new physics effects in  $B \rightarrow X_d \gamma$  and the corresponding two CP asymmetries are very small.

### 7.3 Scenario 2

At first sight one could think that this is another version of the MFV scenario just discussed, but this is not the case. The point is that breaking the degeneracy of mirror fermion masses introduces a new source of flavour violation that has nothing to do with the top Yukawa couplings. Only if accidentally the contributions proportional to  $\xi_3^{(q)}$  dominates the new physics contributions, one would again end up with a scenario that effectively looks like MFV. However, as the mirror spectrum is generally different from the quark spectrum and not as hierarchical as the latter one, the terms involving  $\xi_2^{(q)}$  in the formulae (3.17)-(3.21), (4.8) and (4.9) cannot be neglected although this can be done in the T-even contributions. As the phases in  $\lambda_c^{(q)}$  are different from the ones in  $\lambda_t^{(q)}$ , that dominate the SM contributions, even in this simple scenario the MFV relations in (6.2) will be violated.

The new contributions to particle-antiparticle mixing and  $B \rightarrow X_s \gamma$  are in this scenario entirely dependent on only five parameters

$$x_L, \quad f, \quad m_{H1}, \quad m_{H2}, \quad m_{H3} \quad (7.3)$$

in addition to  $m_t$  and on the CKM parameters that we set to the central values obtained from tree level decays.

Our numerical analysis shows that also in this scenario none of the problems listed in Section 5 can be solved. Still the new physics effects are larger than in the Scenario 1 just discussed. This is shown in Fig. 6 which corresponds to Fig. 5.

We have evaluated the relative deviations of  $\Delta M_s$  and  $Br(B \rightarrow X_s \gamma)$  from their SM values for mirror fermion masses in the range of 300...3000 GeV and for combinations of  $x_L$  and  $f$  allowed by precision electroweak constraints. One finds that the new contributions by the mirror fermions additionally enhance the ratios  $\Delta M_q/(\Delta M_q)_{\text{SM}}$  for all and the ratio  $Br(B \rightarrow X_s \gamma)/Br(B \rightarrow X_s \gamma)_{\text{SM}}$  for most choices of the mirror spectrum. The maximal deviations are 20% and 2% respectively. The new physics effects in  $Br(B \rightarrow X_d \gamma)$  and in  $A_{\text{CP}}(B \rightarrow X_{s,d} \gamma)$  are very small. The only interesting constraint for this choice of  $V_{Hd}$  is the bound on the mass splitting between the first two mirror quark generations coming from  $\Delta M_K$  and  $\varepsilon_K$  as discussed in [28].

## 7.4 Scenario 3

In this scenario, relative to the previous scenarios, there is the first hope that our problems could be solved as the matrix  $V_{Hd}$  now differs from the CKM matrix. In particular

$$S_{\psi K_S} = \sin(2\beta_{\text{true}} + 2\varphi_{B_d}), \quad (7.4)$$

where  $\beta_{\text{true}} = 25.8^\circ$  gives  $S_{\psi K_S} = 0.78$  for  $\varphi_{B_d} = 0$ . Thus in order to fit the experiment we need a small negative phase  $\varphi_{B_d}$ . It turns out that

- In this scenario  $\varphi_{B_d}$  is consistent with all existing constraints in the range of  $[-45^\circ, 45^\circ]$  and it is possible to obtain agreement with the experimental value of  $S_{\psi K_S}$ .
- Interestingly, also in this scenario,  $\Delta M_s \geq (\Delta M_s)_{\text{SM}}$  with maximal deviations from the SM around 15%.  $Br(B \rightarrow X_s \gamma)$  can be enhanced by at most 3% and suppressed by 1%. Similarly to  $Br(B \rightarrow X_s \gamma)$ , the new physics effects in  $B \rightarrow X_d \gamma$  and the corresponding two CP asymmetries are very small.
- CP-violating effects in the  $B_s^0 - \bar{B}_s^0$  system are small since  $\varphi_{B_s}$  is in the ballpark of  $\pm 2^\circ$ .

## 7.5 Scenario 4

We have seen that except for the solution of the “ $R_b - \sin 2\beta$ ” problem in Scenario 3 none of the goals on our list could be reached in the three scenarios considered so far and it is time to modify the mirror fermion spectrum and the structure of the matrix  $V_{Hd}$  in order to make any progress. In particular the CP-violating effects in the  $B_s^0 - \bar{B}_s^0$  system remained small. This is easy to understand. If the matrix  $V_{Hd}$  has a hierarchical structure that is similar to the one of the CKM matrix, the phases of  $\xi_2^{(s)}$  and  $\xi_3^{(s)}$  that

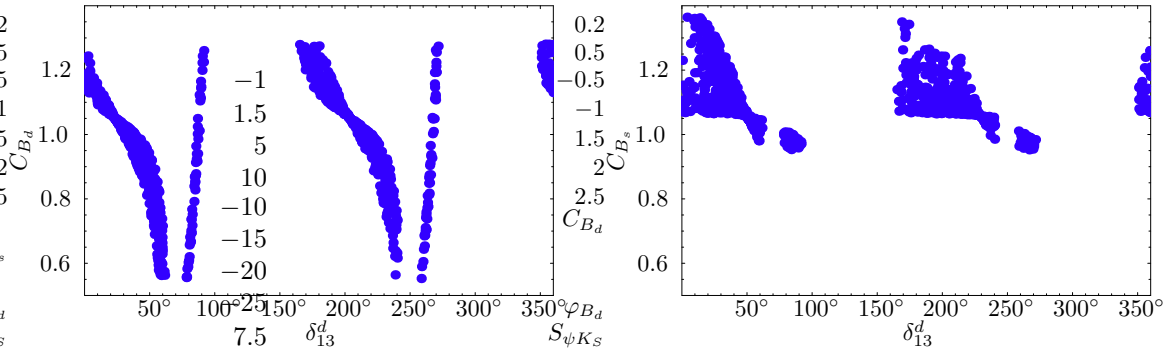


Figure 7:  $C_{B_d}$  and  $C_{B_s}$  as functions of the new phase  $\delta_{13}^d$  in Scenario 4.

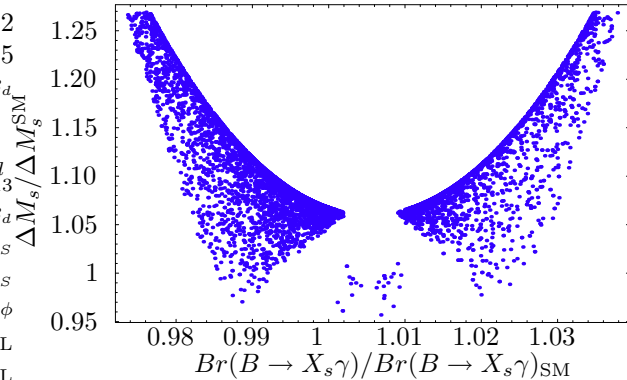


Figure 8: Correlation between  $C_{B_s}$  and  $Br(B \rightarrow X_s \gamma)$  in Scenario 4.

are relevant for CP violation in the  $B_s^0$  system will remain small. In order to obtain large CP-violating effects in this system we have to increase the phases of these two CKM-like factors. While doing this we have to make sure that the known CP-violating effects in the  $B_d^0$  and  $K^0$  systems are still consistent with the data. The case of  $B_d^0$  is not very problematic as the CP-violating effects are large anyway, but due to small experimental values of  $\varepsilon_K$  and  $\Delta M_K$  only for a particular structure of  $V_{Hd}$  we can reach goal 3 without disagreeing with the data on these two observables.

By inspecting the matrix  $V_{Hd}$  in (2.14) we conclude that the mirror fermions in the first two generations have to be almost degenerate in mass in order to satisfy the  $\Delta M_K$  and  $\varepsilon_K$  constraints and simultaneously the mixing parameters in the  $V_{Hd}$  matrix must be in the ranges given in (6.8). This simple procedure turns out to be successful: all our goals can be reached. The most interesting results in this scenario are collected in Figs. 7–11.

In Fig. 7 we show the ratios  $C_{B_d}$  and  $C_{B_s}$  as functions of the new phase  $\delta_{13}^d$ . We observe that only certain ranges of  $\delta_{13}^d$  are allowed. This follows from the experimental constraint on  $S_{\psi K_S}$ . We also observe that while it is easy to obtain values of  $C_{B_d}$  below

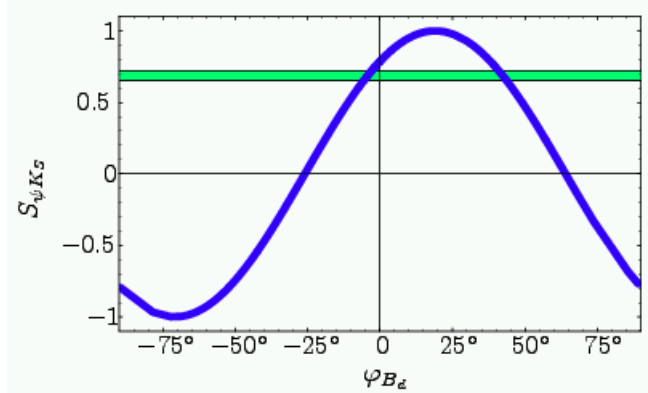


Figure 9:  $S_{\psi K_S}$  as a function of  $\varphi_{B_d}$  in Scenario 4.

unity, this is much harder in the case of  $C_{B_s}$ . Yet a suppression of  $\Delta M_s$  relative to  $(\Delta M_s)_{\text{SM}}$  by  $5 - 10\%$  is possible in this scenario, which should be sufficient to obtain an agreement with experiment if necessary. We observe that the suppression below unity is more likely in the case of  $C_{B_d}$ . The ratio  $C_{B_d}/C_{B_s}$  can deviate from unity even by  $(30 - 40)\%$  so that a relevant violation of the MFV relation between  $\Delta M_s/\Delta M_d$  and  $|V_{ts}/V_{td}|$  as seen in (3.37) is possible.

In Fig. 8 we show the correlation between  $C_{B_s}$  and  $Br(B \rightarrow X_s \gamma)$  normalized to its central SM value. The main message from this plot is that  $Br(B \rightarrow X_s \gamma)$  is changed by at most  $\pm 4\%$  which is welcomed as the SM agrees well with the data. It will be very difficult to distinguish LHT from the SM in this case. New physics effects in  $Br(B \rightarrow X_d \gamma)$  and  $A_{\text{CP}}(B \rightarrow X_{s,d} \gamma)$  are small.

More interesting effects are found in the CP-violating observables related to  $B_d^0 - \bar{B}_d^0$  mixing and in particular to  $B_s^0 - \bar{B}_s^0$  mixing. As already seen in Fig. 7, this scenario is consistent with the data on  $S_{\psi K_S}$  in spite of a large value of  $R_b$ . In order to illustrate this explicitly, we show in Fig. 9  $S_{\psi K_S}$  as a function of  $\varphi_{B_d}$ . To this end we have removed the corresponding experimental constraint but kept the remaining ones. For  $\varphi_{B_d} \approx -3^\circ$  and  $\varphi_{B_d} \approx 43^\circ$  agreement with experiment can be obtained. We will see below that the second solution although not ruled out is not favoured by the data on  $A_{\text{SL}}^d$ . At present, therefore, the cosine measurement  $\cos(2\beta + 2\varphi_{B_d}) = 1.69 \pm 0.67$  [67] represents the strongest constraint in disfavouring the solution  $\varphi_{B_d} = 43^\circ$ .

While this result is clearly interesting, an even more impressive result is shown in the left panel of Fig. 10, where we plot  $A_{\text{SL}}^s$  normalized to its SM central value versus  $S_{\psi\phi}$ . Comparing this plot with the corresponding plot in [39], where the correlation between  $A_{\text{SL}}^s$  and  $S_{\psi\phi}$  has been pointed out, we observe that in a specific model like the one considered here, the correlation in question is much stronger than in a model independent approach considered in that paper. This plot shows that  $S_{\psi\phi}$  can be as large

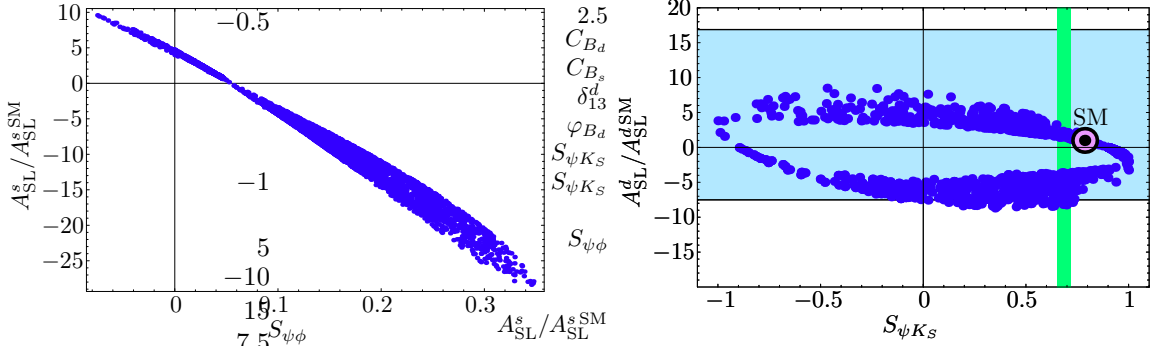


Figure 10:  $A_{SL}^s$  and  $A_{SL}^d$  as functions of  $S_{\psi\phi}$  and  $S_{\psi K_S}$ , respectively, in Scenario 4. The shaded areas represent the experimental data.

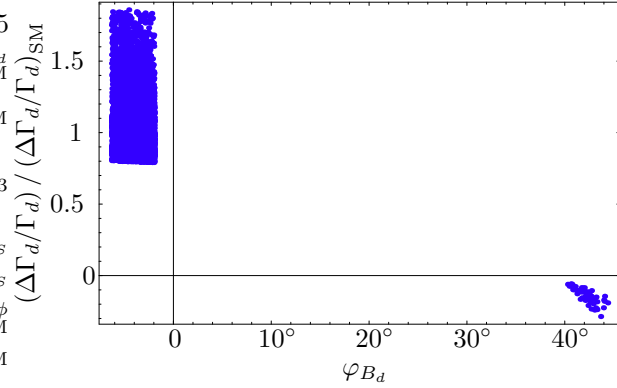


Figure 11:  $\Delta\Gamma_d/\Gamma_d$  as a function of  $\varphi_{B_d}$  in Scenario 4.

as  $+0.30$  and the absolute value of the asymmetry  $A_{SL}^s$  can be enhanced by a factor of  $10 - 20$  relative to the SM value. While both asymmetries can have both signs,  $S_{\psi\phi} > 0$  and  $A_{SL}^s < 0$  seem to be more likely, which implies the preference for a *negative* phase  $\varphi_{B_s}$ . The present data are not yet conclusive but the analysis in [53] indicates that this sign is also favoured by the data on  $A_{SL}^s$ .

In the right panel of Fig. 10 we show  $A_{SL}^d$  normalized to its SM value versus  $S_{\psi K_S}$ . As the latter asymmetry is already well measured, the new physics effects are much more constrained than in the case of  $A_{SL}^s$ . Still an enhancement by a factor of 3 for the case of  $\varphi_{B_d} \approx -3^\circ$  is possible. On the other hand as seen in Fig. 10 for the  $\varphi_{B_d} \approx 43^\circ$  solution the asymmetry in question changes sign relatively to the SM value and its magnitude can be enhanced by a factor of seven, which could soon be ruled out with improved data.

Finally, in Fig. 11 we show  $\Delta\Gamma_d/\Gamma_d$  versus  $\varphi_{B_d}$ . The experimental error in (3.50) is so large that nothing conclusive can be said at present. The future improved data could help to distinguish between the two solutions for  $\varphi_{B_d}$ . In the case of  $\Delta\Gamma_s/\Gamma_s$ , the SM value, that is below the experimental data, is further suppressed for  $\varphi_{B_s} \neq 0$ , but even

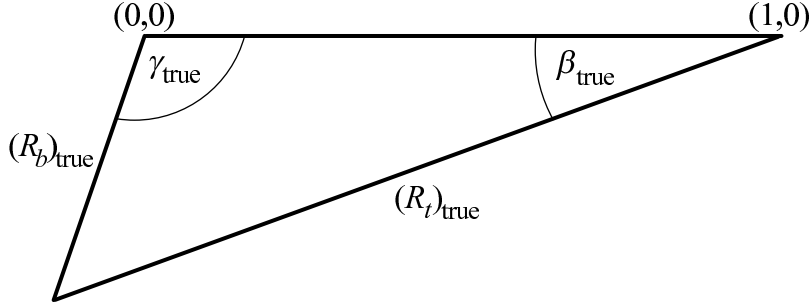


Figure 12: “Upside-down” unitarity triangle in Scenario 5.

for  $\varphi_{B_s} = -8^\circ$  corresponding to  $S_{\psi\phi} = 0.30$ , this suppression amounts to 5%. Improved data and the theory for  $\Delta\Gamma_s$  will tell us how large the phase  $\varphi_{B_s}$  and the asymmetry  $S_{\psi\phi}$  can be.

## 7.6 Scenario 5

Using the central value for  $\gamma$  in the second solution in (7.1) and the central value of  $|V_{ub}|$  in Table 1 we find by means of (5.5)

$$(R_t)_{\text{true}} = 1.217, \quad \beta_{\text{true}} = -20.0^\circ, \quad (7.5)$$

and consequently within the SM approximately opposite signs for  $\varepsilon_K$  and  $S_{\psi K_S}$  compared with the data:

$$\varepsilon_K = -3.72 \cdot 10^{-3} e^{i\pi/4}, \quad S_{\psi K_S} = -0.643. \quad (7.6)$$

The corresponding unitarity triangle is shown in Fig. 12.

In order to obtain agreement with the data we need positive new physics contributions in both cases that are in magnitude by a factor of three and two, respectively, larger than the SM contribution. On the other hand  $\Delta M_d$  turns out to be too large

$$\Delta M_d = 0.904/\text{ps}. \quad (7.7)$$

The question then arises whether one could still modify all these values with the help of mirror fermions. As now a very large *positive* phase  $\varphi_{B_d}$  is required to fit the experimental value of  $S_{\psi K_S}$ , it will be interesting to see how  $\Delta\Gamma_q$  given in (3.52) is modified relatively to the SM value.

The most interesting results in this scenario, related to the  $B_d^0 - \bar{B}_d^0$  system, are shown in Figs. 13–16.

As already stated in the previous section, in this scenario the CP-violating effects in the  $B_s^0 - \bar{B}_s^0$  system are very small. It also turns out that in this scenario  $\Delta M_s$  cannot be suppressed relative to the SM. On the other hand as clearly seen in Fig. 13, where

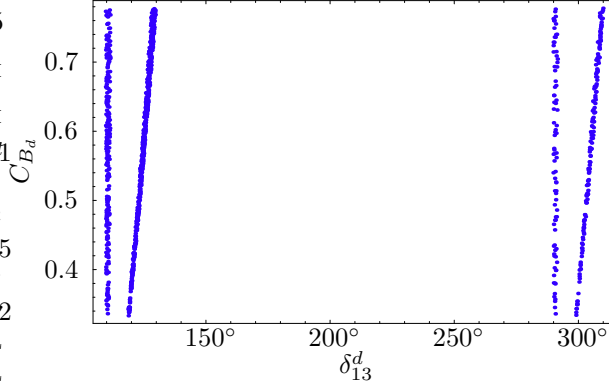


Figure 13:  $C_{B_d}$  as a function of  $\delta_{13}^d$  in Scenario 5.

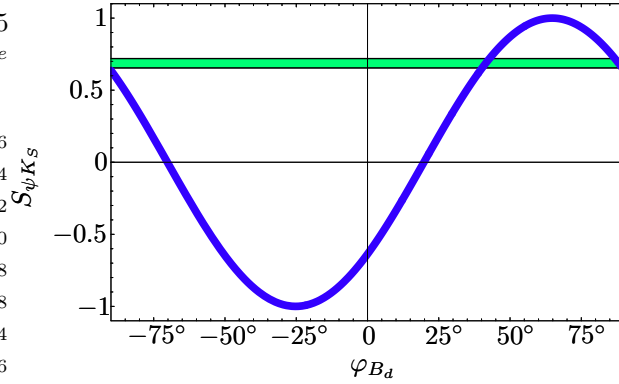


Figure 14:  $S_{\psi K_S}$  as a function of  $\varphi_{B_d}$  in Scenario 5.

we plot  $C_{B_d}$  versus  $\delta_{13}^d$ ,  $C_{B_d}$  can be suppressed below unity bringing  $\Delta M_d$  to agree with experiment.

The CP-violating new physics effects in the  $B_d^0 - \bar{B}_d^0$  system are spectacular in this scenario because the phase  $\varphi_{B_d}$  must take a value in the ballpark of  $42^\circ$  or  $88^\circ$  in order to fit the experimental value of  $S_{\psi K_S}$ . We show this in Fig. 14.

In turn the large value of  $\varphi_{B_d}$  has a large impact on  $A_{\text{SL}}^d$  and  $\Delta\Gamma_d$ . This study requires, however, some care. The point is that with the value  $\gamma = -109^\circ$ , also the values in (3.46) and (3.47) change. We find now

$$\text{Re} \left( \frac{\Gamma_{12}^d}{M_{12}^d} \right) = -(3.4 \pm 1.0) \cdot 10^{-3}, \quad \text{Re} \left( \frac{\Gamma_{12}^s}{M_{12}^s} \right) = -(2.6 \pm 1.0) \cdot 10^{-3}, \quad (7.8)$$

$$\text{Im} \left( \frac{\Gamma_{12}^d}{M_{12}^d} \right) = +(3.8 \pm 0.8) \cdot 10^{-4}, \quad \text{Im} \left( \frac{\Gamma_{12}^s}{M_{12}^s} \right) = -(3.2 \pm 0.6) \cdot 10^{-5}, \quad (7.9)$$

In Fig. 15 we show  $A_{\text{SL}}^d$  as a function of  $S_{\psi K_S}$  normalized to the central SM value in (3.49). The solution with large values of  $A_{\text{SL}}^d$  in Fig. 15 corresponds to  $\varphi_{B_d} \approx 42^\circ$  and is

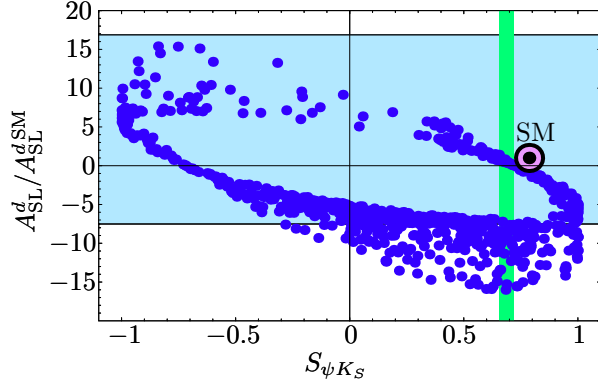


Figure 15:  $A_{\text{SL}}^d$  as a function of  $S_{\psi K_S}$  in Scenario 5. The shaded area represents the experimental data.

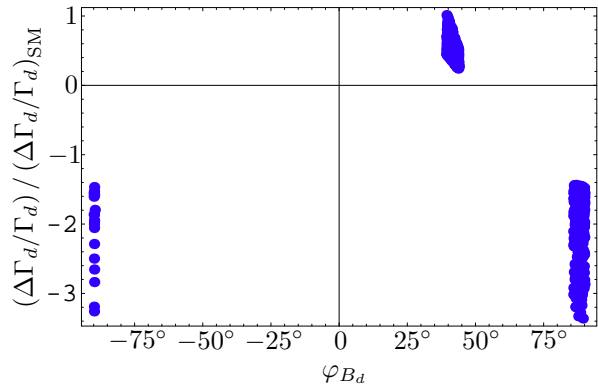


Figure 16:  $\Delta\Gamma_d / \Gamma_d$  as a function of  $\varphi_{B_d}$  in Scenario 5.

by an order of magnitude larger than the SM predictions and has the opposite sign. We would like to stress that, being  $\beta = -20.0^\circ$  in this scenario, this is the solution strongly favoured by the cosine measurement  $\cos(2\beta + 2\varphi_{B_d}) = 1.69 \pm 0.67$  [67]. Therefore, more accurate measurements of the semileptonic asymmetry  $A_{\text{SL}}^d$  could soon rule out the  $\varphi_{B_d} \approx 42^\circ$  solution and, when combined with the cosine measurement, the whole scenario 5.

In Fig. 16 we show  $\Delta\Gamma_d / \Gamma_d$  as a function of  $\varphi_{B_d}$  normalized to the SM value in (3.48). The large experimental errors do not allow to exclude any of these solutions at present.

The new physics effects in  $B \rightarrow X_{s,d}\gamma$  are very small. However as  $\gamma$  has been changed to  $-109^\circ$  in the SM contributions, the final results differ from the SM expectations.  $Br(B \rightarrow X_s\gamma)$  is suppressed by roughly 4% and  $Br(B \rightarrow X_d\gamma)$  enhanced by roughly a factor of two.  $A_{\text{CP}}(B \rightarrow X_d\gamma)$  is changed from  $-10\%$  to  $+5\%$  which could in principle be used to confirm or rule out this scenario. On the other hand  $A_{\text{CP}}(B \rightarrow X_s\gamma)$  changes sign but remains of the same size as in the SM.

## 7.7 Comparison of various Scenarios

The messages from this analysis are as follows:

- Scenarios 1 and 2 are not very exciting and both are rather close to the SM expectations. In particular, they do not solve any of the problems listed in Section 5.
- Scenario 3 is capable of solving the “ $R_b - \sin 2\beta$ ” problem but the problems of a too small  $\Delta M_s$  in (5.9) and the smallness of CP-violating effects in the  $B_s^0 - \bar{B}_s^0$  system remain essentially unchanged.
- Scenario 4 appears to be the most interesting one as it offers solutions to all problems and predicts large CP-violating effects in the  $B_s^0 - \bar{B}_s^0$  system. In particular, we find that  $S_{\psi\phi}$  can be as large as 0.30 and  $A_{\text{SL}}^s$  enhanced by more than an order of magnitude above the SM prediction. The plots in Fig. 10 demonstrate it in an impressive manner.
- Scenario 5 is also interesting as the presence of mirror fermions allows for the agreement of the “upside-down” reference unitarity triangle, shown in Fig. 12, with all existing data. We emphasize that in this scenario the asymmetry  $A_{\text{SL}}^d$  has opposite sign to the SM and, as seen in Fig. 15, a more accurate measurement of  $A_{\text{SL}}^d$  could soon rule out this scenario.

## 7.8 Determining the Parameters of the LHT Model

Let us finally outline how in principle the parameters of the LHT model could be determined. We have discussed this already briefly in Section 2.5. Here we will describe it in explicit terms by presenting a four step procedure:

### Step 1

The discovery of one of the gauge bosons  $A_H$ ,  $W_H$ ,  $Z_H$  determines the scale  $f$  and predicts the masses of the remaining two gauge bosons.

### Step 2

The discovery of  $T_+$  or  $T_-$  determines  $x_L$  as  $f$  has been determined above. Knowing  $x_L$  from  $m_{T_-}$  determines  $m_{T_+}$  and vice versa.

### Step 3

The discovery of mirror fermions will provide the masses  $m_{H1}$ ,  $m_{H2}$ ,  $m_{H3}$  and test the near degeneracy of mirror fermions within the  $SU(2)_L$  doublets.

### Step 4

The matrix  $V_{Hd}$  and the unitarity triangles are determined in FCNC processes.

The determination of the four parameters of the  $V_{Hd}$  matrix requires basically four FCNC processes up to discrete ambiguities. As these parameters describe the deviations from the SM results, precise results obtained in the SM are required. From the present perspective, the mass differences  $\Delta M_K$ ,  $\Delta M_d$  and  $\Delta M_s$  being still subjects to significant non-perturbative uncertainties, will not serve us in this decade to achieve this goal. Among the observables related to particle-antiparticle mixing the following four stand out as being very useful

$$\frac{\Delta M_d}{\Delta M_s}, \quad S_{\psi K_S}, \quad S_{\psi \phi}, \quad \varepsilon_K, \quad (7.10)$$

provided the accuracy on the parameters  $\xi$  and in particular  $\hat{B}_K$  will be further improved. Similarly, when the theoretical errors on  $\text{Re}(\Gamma_{12}^q/M_{12}^q)^{\text{SM}}$  decrease with time, the measurements of  $A_{\text{SL}}^q$  will determine the parameters  $C_{B_d}$  and  $C_{B_s}$  as discussed in Section 3.8 and in [37], provided  $S_{\psi K_S}$  and  $S_{\psi \phi}$  will differ significantly from the SM predictions.

Additional information that can be used to determine the  $V_{Hd}$  matrix will come one day from  $Br(B_s \rightarrow \mu^+ \mu^-)$  and  $Br(B_d \rightarrow \mu^+ \mu^-)$ . Their ratio does not depend on weak decay constants [46] and is theoretically rather clean. Similar comments apply to  $Br(B \rightarrow X_{s,d} \nu \bar{\nu})$  and  $Br(B \rightarrow X_{s,d} \ell^+ \ell^-)$ . Finally, at the beginning of the next decade the very clean decays  $K^+ \rightarrow \pi^+ \nu \bar{\nu}$  and  $K_L \rightarrow \pi^0 \nu \bar{\nu}$  and useful decays  $K_L \rightarrow \pi^0 \ell^+ \ell^-$  could provide decisive tests of the LHT model.

## 8 $D^0 - \bar{D}^0$ Mixing

$D^0 - \bar{D}^0$  mixing in the SM has a very different structure from  $K^0 - \bar{K}^0$  and  $B_q^0 - \bar{B}_q^0$  mixings. Here the quarks running in box diagrams are the down-type quarks implying that the short distance part of  $\Delta M_D$  is very strongly suppressed in the SM by GIM. As a result of this structure,  $\Delta M_D$  in the SM is dominated by the long distance contributions and unless new physics contributions are very large,  $\Delta M_D$  does not provide a useful constraint.

In the LHT model the T-even contributions to  $\Delta M_D$  can be neglected with the same argument as the SM contributions. Also tree level effects, which appear due to the modified flavour structure in the up-type quark sector, relatively to the SM, can be neglected, as shown in [80]. On the other hand, as already analyzed in [28], the mirror fermions could have a significant impact on  $\Delta M_D$ .

The effective Hamiltonian for the mirror fermion contribution to the  $D^0 - \bar{D}^0$  system

can be obtained from the  $\Delta S = 2$  Hamiltonian in (3.14) with the following replacements:

$$\xi_i \rightarrow \xi_i^{(D)} = V_{Hu}^{ui} {}^* V_{Hu}^{ci}, \quad \sum_i \xi_i^{(D)} = 0, \quad (8.1)$$

$$(\bar{s}d)_{V-A} (\bar{s}d)_{V-A} \rightarrow (\bar{c}u)_{V-A} (\bar{c}u)_{V-A}. \quad (8.2)$$

Therefore, in (3.17) also the replacements

$$F_K \rightarrow F_D, \quad \hat{B}_K \rightarrow \hat{B}_D, \quad m_K \rightarrow m_D, \quad (8.3)$$

have to be made. The QCD correction is approximately equal to  $\eta_2$ . Although the role of up mirror fermions and down mirror fermions is now interchanged, with down mirror fermions accompanied by  $W_H^\pm$  and up mirror fermions accompanied by  $Z_H$  and  $A_H$  in box diagrams, no change in (3.18), except for (8.1), has to be made, because of the equality of the masses of up and down mirror fermions belonging to a given  $SU(2)_L$  doublet.

The current experimental bound on  $D^0 - \bar{D}^0$  mixing is given by [77]

$$\Delta M_D = |m_{D_1^0} - m_{D_2^0}| < 4.6 \cdot 10^{-14} \text{ GeV} \quad (95\% \text{ C.L.}). \quad (8.4)$$

A detailed analysis of the implications of this bound on the mass spectrum of mirror fermions has been presented in [28]. We do not want to repeat this analysis here as we basically agree with the results of these authors in this case. In all our numerical results the bound in (8.4) has been taken into account.

## 9 Summary and Outlook

In this paper we have calculated a number of observables related to particle-antiparticle mixing in the Littlest Higgs model (LHT) with T-parity. The first analysis of particle-antiparticle mixing in this model has been presented by Hubisz et al. [28]. We confirm the effective Hamiltonian for  $\Delta F = 2$  transitions found by these authors but our phenomenological analysis differs from theirs in various aspects. While Hubisz et al. studied only  $\Delta M_q$  mass differences and  $\varepsilon_K$  with the goal to constrain the mass spectrum and weak mixing matrix of mirror fermions, our main goal was to include in the analysis also most interesting CP-violating observables in  $B_d$  and  $B_s$  decays and to use the new flavour and CP-violating interactions present in the LHT model to remove possible discrepancies between the SM and existing data. Moreover, we have calculated in the LHT model for the first time the branching ratios for the  $B \rightarrow X_{s,d}\gamma$  decays and the related CP asymmetries.

The main messages of our paper are as follows:

- The LHT model can be made consistent with all FCNC processes considered in the present paper for masses of mirror fermions and new weak gauge bosons in the reach of LHC, provided the weak mixing matrix  $V_{Hd}$  exhibits a hierarchical structure and the mass spectrum of mirror fermions is quasi-degenerate.
- We emphasize, however, that the structure of the mixing matrix  $V_{Hd}$  can differ significantly from the known structure of the CKM matrix so that interesting departures from MFV correlations between various processes are possible. Basically all MFV correlations between  $K$ ,  $B_d^0$  and  $B_s^0$  meson systems can be modified, while being still consistent with the existing data, even if these modifications amount to at most 30% in the case of the CP-conserving observables considered here.
- The above size of still possible deviations from the SM implies that the mass differences  $\Delta M_q$  and  $\varepsilon_K$  considered in [28] are not the appropriate observables to identify possible signals from mirror fermions, heavy gauge bosons and  $T_+$ , as the non-perturbative uncertainties in these observables are comparable to the new effects themselves. A good example are the results in (5.8). Certainly,  $\Delta M_q$  and  $\varepsilon_K$  can serve as first tests of the viability of the model but to constrain and test the model in detail, significantly cleaner, from the theoretical point of view, observables have to be considered. These are in particular the mixing induced CP asymmetries  $S_{\psi K_S}$  and  $S_{\psi\phi}$  but also  $\Delta M_d/\Delta M_s$ ,  $A_{\text{SL}}^q$  and  $\Delta\Gamma_q$ . This also applies to  $\text{Br}(B \rightarrow X_{s,d}\gamma)$ , the related CP asymmetries and a number of rare decay branching ratios with the latter considered in a separate paper [36].
- We find that the T-even sector of the LHT model, that represents this model in FCNC processes in the limit of exactly degenerate mirror fermions is not favoured by the data as independently of the parameters of this sector  $\Delta M_s > (\Delta M_s)_{\text{SM}}$  and the possible discrepancy between the value of the CP asymmetry  $S_{\psi K_S}$  and large values of  $|V_{ub}|$  cannot be removed.
- Using the full structure of new flavour and CP-violating interactions encoded in  $V_{Hd} \neq V_{\text{CKM}}$ , we identify regions in the parameter space of the LHT model in which possible problems of the SM can be cured, large CP-violating effects in the  $B_s^0$  system are predicted and the mass difference  $\Delta M_s$  is found to be smaller than  $(\Delta M_s)_{\text{SM}}$  as suggested by the recent result of the CDF collaboration.
- In particular we identify a scenario in which significant enhancements of the CP asymmetries  $S_{\psi\phi}$  and  $A_{\text{SL}}^q$  relative to the SM are possible, while satisfying all existing constraints, in particular from the  $B \rightarrow X_s\gamma$  decay and  $A_{\text{CP}}(B \rightarrow X_s\gamma)$  that are presented in the LHT model here for the first time. In this scenario the

weak mixing matrix of mirror fermions turns out to have a hierarchical structure that differs by much from the CKM one.

- In another scenario the second, non-SM, value for the angle  $\gamma = -(109 \pm 16)^\circ$  from tree level decays can be made consistent with all existing data with the help of mirror fermions.
- We have found a number of correlations between the observables in question and studied the implications of our results for the mass spectrum and the weak mixing matrix of mirror fermions.
- The effects from mirror fermions in the  $B \rightarrow X_s \gamma$  decay turn out to be smaller than in the  $\Delta B = 2$  transitions, which should be welcomed as the SM is here in a rather good shape. Typically the new physics effects are below 4%.
- We also find that the new physics effects in  $A_{\text{CP}}(B \rightarrow X_{s,d} \gamma)$  are very small but their measurements could in principle help to rule out the  $\gamma = -109^\circ$  solution from tree level decays, as  $A_{\text{CP}}(B \rightarrow X_{s,d} \gamma)$  reverses its sign. A similar comment applies to  $A_{\text{SL}}^q$ .

## Acknowledgments

We would like to thank Marcella Bona, Gino Isidori and Luca Silvestrini for useful discussions and Stefan Recksiegel for a careful reading of the paper. A.J.B. and A.W. would also like to thank Luca Silvestrini and INFN for the hospitality at the University of Rome “La Sapienza”, where the final steps of this paper have been made. This research was partially supported by the German ‘Bundesministerium für Bildung und Forschung’ under contract 05HT4WOA/3.

## A Non-leading Contributions of $T_-$ and $\Phi$

Here we want to demonstrate explicitly that the T-odd heavy  $T_-$  does not contribute to any of the processes we study and that the heavy scalar triplet  $\Phi$  does not contribute at  $\mathcal{O}(v^2/f^2)$ . The reasons are as follows:

- Omitting the first two quark generations, the masses for  $t$ ,  $T_+$  and  $T_-$  are generated through the following Yukawa interaction [23, 25]:

$$\begin{aligned} \mathcal{L}_{\text{top}} = & -\frac{1}{2\sqrt{2}}\lambda_1 f \epsilon_{ijk} \epsilon_{xy} \left[ (\bar{Q}_1)_i (\Sigma)_{jx} (\Sigma)_{ky} - (\bar{Q}_2 \Sigma_0)_i (\tilde{\Sigma})_{jx} (\tilde{\Sigma})_{ky} \right] t_R \\ & - \lambda_2 f (\bar{t}'_1 t'_{1R} + \bar{t}'_2 t'_{2R}) + h.c. . \end{aligned} \quad (\text{A.1})$$

This leads to a mixing between the weak eigenstates of  $t$  and  $T_+$ , and therefore, couplings of the form  $\bar{T}_+ W_L^+ d^i$  exist. They are suppressed by  $v/f$ , as the mixing appears only at this order.

- However,  $u_H^3$ , as all other mirror fermions, gets its mass from the Dirac mass term (omitting again the first two generations) [25]

$$\mathcal{L}_{\text{Dirac}} = -\kappa f (\bar{\Psi}_2 \xi \Psi_R + \bar{\Psi}_1 \Sigma_0 \Omega \xi^\dagger \Omega \Psi_R) + h.c. \quad (\text{A.2})$$

so that there is no tree level mixing of  $T_-$  with  $u_H^3$  (and the other mirror quarks). Therefore,  $T_-$  stays singlet under  $SU(2)_1 \times SU(2)_2$  and does not couple to ordinary down-type quarks. Thus  $T_-$  does not contribute neither to  $\Delta B = 2$  and  $\Delta S = 2$  processes nor to  $B \rightarrow X_s \gamma$ .

- The case of  $D^0 - \bar{D}^0$  mixing is slightly more involved. Here,  $T_-$  could contribute via interactions  $\bar{q} A_H T_-$  and  $\bar{q} Z_H T_-$  ( $q = u, c$ ):  $T_-$  couples to the weak eigenstate of  $T_+$  through the interaction with  $B_H$ . As  $T_+$  gets its mass from the up-type Yukawa term (A.1), which also generates the masses of the three up-type quarks, it can in principle mix with all three of them, as pointed out in [80]. However, as found there, this mixing is highly constrained for the first two generations, so we can safely neglect it. In this approximation, there are thus no couplings of the form  $\bar{q} A_H T_-$  and  $\bar{q} Z_H T_-$  ( $q = u, c$ ).
- In summary we find that  $T_-$  has a sizable flavour changing coupling only to  $t$ , thus confirming the corresponding statement made in [28].

For completeness, we also have to consider the contributions of the scalar triplet  $\Phi$  to the processes analyzed in the present paper. The relevant diagrams can be obtained by simply replacing  $W_H^\pm$  by  $\phi^\pm$  and  $A_H$ ,  $Z_H$  by  $\phi^0$ ,  $\phi^P$  in the diagrams shown in Figs. 1

and 3. However, all couplings of  $\Phi$  to fermions turn out to be  $\mathcal{O}(v/f)$ , so that the effect of those diagrams is of higher order in  $v/f$  than the one resulting from diagrams with gauge boson exchanges. Therefore the scalar triplet  $\Phi$  does not contribute at  $\mathcal{O}(v^2/f^2)$  to the processes in question in the LHT model.

## B Relevant Functions

In this Appendix we list the functions that entered the present study of  $\Delta F = 2$  and  $B \rightarrow X_s \gamma$  processes. Both the SM contributions and the new physics contributions coming from the T-even and T-odd sectors are collected. The variables are defined as follows:

$$\begin{aligned} x_q &= \frac{m_q^2}{M_{W_L}^2}, & x_T &= \frac{m_{T+}^2}{M_{W_L}^2} \quad (q = c, t), \\ z_i &= \frac{m_{Hi}^2}{M_{W_H}^2}, & z'_i &= \frac{m_{Hi}^2}{M_{A_H}^2} = z_i a \quad \text{with} \quad a = \frac{5}{\tan^2 \theta_W} \quad (i = 1, 2, 3). \end{aligned} \quad (\text{B.1})$$

### B.1 Functions entering $\Delta F = 2$ Processes

$$S_0(x_t) = \frac{x_t (4 - 11 x_t + x_t^2)}{4 (-1 + x_t)^2} + \frac{3 x_t^3 \log x_t}{2 (-1 + x_t)^3} \quad (\text{B.2})$$

$$\begin{aligned} S_0(x_c, x_t) &= \frac{-3 x_t x_c}{4(-1 + x_t)(-1 + x_c)} - \frac{x_t (4 - 8 x_t + x_t^2) x_c \log x_t}{4(-1 + x_t)^2 (-x_t + x_c)} \\ &+ \frac{x_t x_c (4 - 8 x_c + x_c^2) \log x_c}{4(-1 + x_c)^2 (-x_t + x_c)} \end{aligned} \quad (\text{B.3})$$

$$\begin{aligned} P_1(x_t, x_T) &= \frac{x_t (-4 + 11 x_t - x_t^2 + x_T - 8 x_t x_T + x_t^2 x_T)}{4(-1 + x_t)^2 (-1 + x_T)} + \frac{x_t x_T (4 - 8 x_T + x_T^2) \log x_T}{4(x_t - x_T)(-1 + x_T)^2} \\ &- \frac{x_t (-6 x_t^3 - 4 x_T + 12 x_t x_T - 3 x_t^2 x_T + x_t^3 x_T) \log x_t}{4(-1 + x_t)^3 (x_t - x_T)} \end{aligned} \quad (\text{B.4})$$

$$\begin{aligned} P_2(x_c, x_t, x_T) &= \frac{3(x_t x_c - x_T x_c)}{4(-1 + x_t)(-1 + x_T)(-1 + x_c)} + \frac{(4 x_t x_c - 8 x_t^2 x_c + x_t^3 x_c) \log x_t}{4(-1 + x_t)^2 (x_t - x_c)} \\ &+ \frac{(4 x_t x_c^2 - 4 x_T x_c^2 - 8 x_t x_c^3 + 8 x_T x_c^3 + x_t x_c^4 - x_T x_c^4) \log x_c}{4(x_t - x_c)(x_T - x_c)(-1 + x_c)^2} \\ &- \frac{(4 x_T x_c - 8 x_T^2 x_c + x_T^3 x_c) \log x_T}{4(-1 + x_T)^2 (x_T - x_c)} \end{aligned} \quad (\text{B.5})$$

$$F(z_i, z_j; W_H) = \frac{1}{(1-z_i)(1-z_j)} \left( 1 - \frac{7}{4} z_i z_j \right) + \frac{z_i^2 \log z_i}{(z_i - z_j)(1-z_i)^2} \left( 1 - 2z_j + \frac{z_i z_j}{4} \right) - \frac{z_j^2 \log z_j}{(z_i - z_j)(1-z_j)^2} \left( 1 - 2z_i + \frac{z_i z_j}{4} \right) \quad (\text{B.6})$$

$$G(z_i, z_j; Z_H) = -\frac{3}{4} \left[ \frac{1}{(1-z_i)(1-z_j)} + \frac{z_i^2 \log z_i}{(z_i - z_j)(1-z_i)^2} - \frac{z_j^2 \log z_j}{(z_i - z_j)(1-z_j)^2} \right] \quad (\text{B.7})$$

$$A_1(z_i, z_j; Z_H) = -\frac{3}{100a} \left[ \frac{1}{(1-z'_i)(1-z'_j)} + \frac{z'_i z_i \log z'_i}{(z_i - z_j)(1-z'_i)^2} - \frac{z'_j z_j \log z'_j}{(z_i - z_j)(1-z'_j)^2} \right] \quad (\text{B.8})$$

$$A_2(z_i, z_j; Z_H) = -\frac{3}{10} \left[ \frac{\log a}{(a-1)(1-z'_i)(1-z'_j)} + \frac{z_i^2 \log z_i}{(z_i - z_j)(1-z_i)(1-z'_i)} - \frac{z_j^2 \log z_j}{(z_i - z_j)(1-z_j)(1-z'_j)} \right], \quad (\text{B.9})$$

## B.2 Functions entering $B \rightarrow X_s \gamma$

$$D'_0(y) = -\frac{(3y^3 - 2y^2)}{2(y-1)^4} \log y + \frac{(8y^3 + 5y^2 - 7y)}{12(y-1)^3} \quad (\text{B.10})$$

$$E'_0(y) = \frac{3y^2}{2(y-1)^4} \log y + \frac{(y^3 - 5y^2 - 2y)}{4(y-1)^3} \quad (y = x_t, x_T, z_i, z'_i) \quad (\text{B.11})$$

## References

- [1] See review by H. E. Haber in S. Eidelman *et al.* [Particle Data Group], Phys. Lett. B **592** (2004) 1 and references therein.
- [2] N. Arkani-Hamed, A. G. Cohen and H. Georgi, Phys. Rev. Lett. **86** (2001) 4757 [arXiv:hep-th/0104005]; Phys. Lett. B **513** (2001) 232 [arXiv:hep-ph/0105239].
- [3] For a recent review and a comprehensive collection of references, see:  
M. Schmaltz and D. Tucker-Smith, arXiv:hep-ph/0502182.  
M. Perelstein, arXiv:hep-ph/0512128.
- [4] N. Arkani-Hamed, S. Dimopoulos and G. R. Dvali, Phys. Lett. B **429** (1998) 263 [arXiv:hep-ph/9803315]; I. Antoniadis, N. Arkani-Hamed, S. Dimopoulos and

G. R. Dvali, Phys. Lett. B **436** (1998) 257 [arXiv:hep-ph/9804398]; D. Cremades, L. E. Ibanez and F. Marchesano, Nucl. Phys. B **643** (2002) 93 [arXiv:hep-th/0205074]; C. Kokorelis, Nucl. Phys. B **677** (2004) 115 [arXiv:hep-th/0207234].

[5] L. Randall and R. Sundrum, Phys. Rev. Lett. **83** (1999) 3370 [arXiv:hep-ph/9905221].

[6] N. S. Manton, Nucl. Phys. B **158** (1979) 141; D. B. Fairlie, Phys. Lett. B **82** (1979) 97; J. Phys. G **5** (1979) L55; P. Forgacs, N. S. Manton, Commun. Math. Phys. **72** (1980) 15; G. Chapline, R. Slansky, Nucl. Phys. B **209** (1982) 461; S. Randjbar-Daemi, A. Salam, J. Strathdee, Nucl. Phys. B **214** (1983) 491; N. V. Krasnikov, Phys. Lett. B **273** (1991) 246; D. Kapetanakis and G. Zoupanos, Phys. Rept. **219** (1992) 1.

[7] For an overview of the recent progress in flat space, see for example M. Quiros, arXiv:hep-ph/0302189; and C. A. Scrucca, M. Serone and L. Silvestrini, Nucl. Phys. B **669** (2003) 128 [arXiv:hep-ph/0304220]; and references therein. For the AdS case see, G. Burdman and Y. Nomura, Phys. Rev. D **69** (2004) 115013 [arXiv:hep-ph/0312247]; R. Contino, Y. Nomura and A. Pomarol, Nucl. Phys. B **671** (2003) 148 [arXiv:hep-ph/0306259]; K. y. Oda and A. Weiler, Phys. Lett. B **606** (2005) 408 [arXiv:hep-ph/0410061]; K. Agashe, R. Contino and A. Pomarol, Nucl. Phys. B **719** (2005) 165 [arXiv:hep-ph/0412089]; Y. Hosotani, S. Noda, Y. Sakamura and S. Shimasaki, arXiv:hep-ph/0601241.

[8] S. Weinberg, Phys. Rev. D **13**, (1976) 974; Phys. Rev. D **19**, (1979) 1277; L. Susskind, Phys. Rev. D **20**, (1979) 2619.

[9] For a review, see C. T. Hill and E. H. Simmons, Phys. Rept. **381** (2003) 235 [Erratum-ibid. **390** (2004) 553] [arXiv:hep-ph/0203079].

[10] C. T. Hill, Phys. Lett. B **266** (1991) 419; C. T. Hill, Phys. Lett. B **345** (1995) 483 [arXiv:hep-ph/9411426]; K. D. Lane and E. Eichten, Phys. Lett. B **352** (1995) 382 [arXiv:hep-ph/9503433].

[11] N. Arkani-Hamed, A. G. Cohen, E. Katz and A. E. Nelson, JHEP **0207** (2002) 034 [arXiv:hep-ph/0206021].

[12] T. Han, H. E. Logan, B. McElrath and L. T. Wang, Phys. Rev. D **67** (2003) 095004 [arXiv:hep-ph/0301040].

[13] C. Csaki, J. Hubisz, G. D. Kribs, P. Meade and J. Terning, Phys. Rev. D **67** (2003) 115002 [arXiv:hep-ph/0211124].

- [14] J. L. Hewett, F. J. Petriello and T. G. Rizzo, JHEP **0310** (2003) 062 [arXiv:hep-ph/0211218].
- [15] M. C. Chen and S. Dawson, Phys. Rev. D **70** (2004) 015003 [arXiv:hep-ph/0311032]; arXiv:hep-ph/0409163.
- [16] C. x. Yue and W. Wang, Nucl. Phys. B **683** (2004) 48 [arXiv:hep-ph/0401214].
- [17] W. Kilian and J. Reuter, Phys. Rev. D **70** (2004) 015004 [arXiv:hep-ph/0311095].
- [18] T. Han, H. E. Logan, B. McElrath and L. T. Wang, Phys. Lett. B **563** (2003) 191 [arXiv:hep-ph/0302188].
- [19] A. J. Buras, A. Poschenrieder and S. Uhlig, Nucl. Phys. B **716** (2005) 173 [arXiv:hep-ph/0410309].
- [20] S. R. Choudhury, N. Gaur, A. Goyal and N. Mahajan, arXiv:hep-ph/0407050.
- [21] A. J. Buras, A. Poschenrieder and S. Uhlig, arXiv:hep-ph/0501230.
- [22] W. j. Huo and S. h. Zhu, Phys. Rev. D **68** (2003) 097301 [arXiv:hep-ph/0306029].
- [23] H. C. Cheng and I. Low, JHEP **0309** (2003) 051 [arXiv:hep-ph/0308199]; JHEP **0408** (2004) 061 [arXiv:hep-ph/0405243].
- [24] J. Hubisz, P. Meade, A. Noble and M. Perelstein, JHEP **0601** (2006) 135 [arXiv:hep-ph/0506042].
- [25] I. Low, JHEP **0410** (2004) 067 [arXiv:hep-ph/0409025].
- [26] H. C. Cheng, I. Low and L. T. Wang, arXiv:hep-ph/0510225.
- [27] J. Hubisz and P. Meade, Phys. Rev. D **71** (2005) 035016 [arXiv:hep-ph/0411264].
- [28] J. Hubisz, S. J. Lee and G. Paz, arXiv:hep-ph/0512169.
- [29] G. Gomez-Ceballos [CDF Collaboration], Talk given at FPCP 2006, <http://fpcp2006.triumf.ca/talks/day3/1500/fpcp2006.pdf>.
- [30] V. Abazov [DØ Collaboration], arXiv:hep-ex/0603029.
- [31] A. J. Buras, P. Gambino, M. Gorbahn, S. Jager and L. Silvestrini, Phys. Lett. B **500** (2001) 161 [arXiv:hep-ph/0007085]. A. J. Buras, Acta Phys. Polon. B **34** (2003) 5615 [arXiv:hep-ph/0310208].

- [32] G. D'Ambrosio, G. F. Giudice, G. Isidori and A. Strumia, Nucl. Phys. B **645** (2002) 155 [arXiv:hep-ph/0207036].
- [33] For earlier discussions of the MFV hypothesis see: R. S. Chivukula and H. Georgi, Phys. Lett. B **188** (1987) 99. L. J. Hall and L. Randall, Phys. Rev. Lett. **65** (1990) 2939.
- [34] A. J. Buras, R. Fleischer, S. Recksiegel and F. Schwab, Nucl. Phys. B **697** (2004) 133 [arXiv:hep-ph/0402112].
- [35] K. Agashe, M. Papucci, G. Perez and D. Pirjol, arXiv:hep-ph/0509117.
- [36] M. Blanke, A. J. Buras, A. Poschenrieder, C. Tarantino, S. Uhlig and A. Weiler, in preparation.
- [37] M. Blanke, A. J. Buras, D. Guadagnoli and C. Tarantino, arXiv:hep-ph/0604057.
- [38] M. Bona *et al.* [UTfit Collaboration], arXiv:hep-ph/0509219; arXiv:hep-ph/0605213. <http://utfit.roma1.infn.it>.
- [39] Z. Ligeti, M. Papucci and G. Perez, arXiv:hep-ph/0604112.
- [40] P. Ball and R. Fleischer, arXiv:hep-ph/0604249.
- [41] S. Khalil, arXiv:hep-ph/0605021.
- [42] Y. Grossman, Y. Nir and G. Raz, arXiv:hep-ph/0605028.
- [43] A. Datta, arXiv:hep-ph/0605039.
- [44] B. Pontecorvo, Sov. Phys. JETP **6** (1957) 429 [Zh. Eksp. Teor. Fiz. **33** (1957) 549]; Sov. Phys. JETP **7** (1958) 172 [Zh. Eksp. Teor. Fiz. **34** (1957) 247]; Z. Maki, M. Nakagawa and S. Sakata, Prog. Theor. Phys. **28** (1962) 870.
- [45] N. Cabibbo, Phys. Rev. Lett. **10** (1963) 531 . M. Kobayashi and T. Maskawa, Prog. Theor. Phys. **49** (1973) 652.
- [46] A. J. Buras, Phys. Lett. B **566** (2003) 115 [arXiv:hep-ph/0303060].
- [47] S. Bergmann and G. Perez, Phys. Rev. D **64** (2001) 115009 [arXiv:hep-ph/0103299].
- [48] A. J. Buras, arXiv:hep-ph/9806471.

- [49] A. J. Buras, M. Jamin and P. H. Weisz, Nucl. Phys. B **347** (1990) 491; J. Urban, F. Krauss, U. Jentschura and G. Soff, Nucl. Phys. B **523** (1998) 40 [arXiv:hep-ph/9710245].
- [50] S. Herrlich and U. Nierste, Nucl. Phys. B **419** (1994) 292 [arXiv:hep-ph/9310311].
- [51] S. Herrlich and U. Nierste, Phys. Rev. D **52** (1995) 6505 [arXiv:hep-ph/9507262]; S. Herrlich and U. Nierste, Nucl. Phys. B **476** (1996) 27 [arXiv:hep-ph/9604330].
- [52] J. Charles *et al.* [CKMfitter Group], Eur. Phys. J. C **41** (2005) 1 [arXiv:hep-ph/0406184], <http://www.slac.stanford.edu/xorg/ckmfitter/>.
- [53] Y. Grossman, Y. Nir and M. P. Worah, Phys. Lett. B **407** (1997) 307 [arXiv:hep-ph/9704287].
- [54] D. Becirevic, V. Gimenez, G. Martinelli, M. Papinutto and J. Reyes, JHEP **0204** (2002) 025 [arXiv:hep-lat/0110091].
- [55] V. Gimenez and J. Reyes, Nucl. Phys. Proc. Suppl. **94** (2001) 350 [arXiv:hep-lat/0010048].
- [56] S. Hashimoto, K. I. Ishikawa, T. Onogi, M. Sakamoto, N. Tsutsui and N. Yamada, Phys. Rev. D **62** (2000) 114502 [arXiv:hep-lat/0004022].
- [57] S. Aoki *et al.* [JLQCD Collaboration], Phys. Rev. D **67** (2003) 014506 [arXiv:hep-lat/0208038].
- [58] D. Becirevic, D. Meloni, A. Retico, V. Gimenez, V. Lubicz and G. Martinelli, Eur. Phys. J. C **18** (2000) 157 [arXiv:hep-ph/0006135].
- [59] L. Lellouch and C. J. D. Lin [UKQCD Collaboration], Phys. Rev. D **64** (2001) 094501 [arXiv:hep-ph/0011086].
- [60] N. Yamada *et al.* [JLQCD Collaboration], Nucl. Phys. Proc. Suppl. **106** (2002) 397 [arXiv:hep-lat/0110087].
- [61] S. Aoki *et al.* [JLQCD Collaboration], Phys. Rev. Lett. **91** (2003) 212001 [arXiv:hep-ph/0307039].
- [62] M. Ciuchini, E. Franco, V. Lubicz, F. Mescia and C. Tarantino, JHEP **0308** (2003) 031 [arXiv:hep-ph/0308029].
- [63] M. Beneke, G. Buchalla, C. Greub, A. Lenz and U. Nierste, Phys. Lett. B **459** (1999) 631 [arXiv:hep-ph/9808385].

- [64] A. S. Dighe, T. Hurth, C. S. Kim and T. Yoshikawa, Nucl. Phys. B **624** (2002) 377 [arXiv:hep-ph/0109088].
- [65] M. Beneke, G. Buchalla, A. Lenz and U. Nierste, Phys. Lett. B **576** (2003) 173 [arXiv:hep-ph/0307344].
- [66] A. Lenz, Talk given at the workshop “Flavour in the era of the LHC”, May 2006, CERN, <http://mlm.home.cern.ch/mlm/FlavLHC.html>.
- [67] The Heavy Flavor Averaging Group (HFAG), <http://www.slac.stanford.edu/xorg/hfag/>.
- [68] R. van Kooten, Talk given at “Flavor Physics & CP Violation”, April 2006, Vancouver, [http://fpcp2006.triumf.ca/talks/day3/1630/FPCP\\_2006\\_talk.pdf](http://fpcp2006.triumf.ca/talks/day3/1630/FPCP_2006_talk.pdf).
- [69] P. Gambino and M. Misiak, Nucl. Phys. B **611** (2001) 338 [arXiv:hep-ph/0104034].
- [70] U. Haisch, Talk given at the workshop “Flavour in the era of the LHC”, May 2006, CERN, <http://mlm.home.cern.ch/mlm/FlavLHC.html>.  
M. Misiak, Talk given at “XLIst Rencontres de Moriond” 2006, <http://moriond.in2p3.fr/QCD/2006/SundayAfternoon/Misiak.pdf>.
- [71] A. L. Kagan and M. Neubert, Phys. Rev. D **58** (1998) 094012 [arXiv:hep-ph/9803368].
- [72] T. Goto, N. Kitazawa, Y. Okada and M. Tanaka, Phys. Rev. D **53** (1996) 6662 [arXiv:hep-ph/9506311]. Y. Grossman, Y. Nir and M. P. Worah, Phys. Lett. B **407** (1997) 307 [arXiv:hep-ph/9704287]. G. Barenboim, G. Eyal and Y. Nir, Phys. Rev. Lett. **83** (1999) 4486. G. Barenboim, G. Eyal and Y. Nir, Phys. Rev. Lett. **83** (1999) 4486 [arXiv:hep-ph/9905397].
- [73] S. Hashimoto, Int. J. Mod. Phys. A **20** (2005) 5133 [arXiv:hep-ph/0411126].
- [74] A. J. Buras, R. Fleischer, S. Recksiegel and F. Schwab, Eur. Phys. J. C **45** (2006) 701 [arXiv:hep-ph/0512032].
- [75] F. J. Botella, G. C. Branco, M. Nebot and M. N. Rebelo, Nucl. Phys. B **725** (2005) 155 [arXiv:hep-ph/0502133].
- [76] E. Blucher *et al.*, arXiv:hep-ph/0512039.
- [77] S. Eidelman *et al.* [Particle Data Group], Phys. Lett. B **592** (2004) 1.
- [78] M. Okamoto, PoS **LAT2005** (2005) 013 [arXiv:hep-lat/0510113].

- [79] S. L. Glashow, J. Iliopoulos and L. Maiani, Phys. Rev. D **2** (1970) 1285.
- [80] J. Y. Lee, JHEP **0412** (2004) 065 [arXiv:hep-ph/0408362].